Geol. Mag. **147** (*3*), *2010, pp. 339–362. © Cambridge University Press 2009*
doi:10.1017/S0016756809990665

Zircon geochronology and trace element characteristics of eclogites and granulites from the Orlica-Śnieżnik complex, Bohemian Massif

MICHAEL BRÖCKER*†, REINER KLEMD‡, ELLEN KOOIJMAN*, JASPER BERNDT* & ALEXANDER LARIONOV§

*Institut für Mineralogie, Universität Münster, Corrensstraße 24, 48149 Münster, Germany
‡GeoZentrum Nordbayern, Universität Erlangen-Nürnberg, Schlossgarten 5a, 91054 Erlangen, Germany
§A. P. Karpinsky All-Russian Geological Research Institute (VSEGEI), Centre of Isotopic Research, Sredny Prospect 74, 199106 St Petersburg, Russia

(*Received* 29 April 2009; *accepted* 29 July 2009; First published online 6 November 2009)

Abstract – U–Pb zircon geochronology and trace element analysis was applied to eclogites and (ultra)high-pressure granulites that occur as volumetrically subordinate rock bodies within orthogneisses of the Orlica-Śnieżnik complex, Bohemian Massif. Under favourable circumstances such data may help to unravel protolith ages and yet-undetermined aspects of the metamorphic evolution, for example, the time span over which eclogite-facies conditions were attained. By means of ion-probe and laser ablation techniques, a comprehensive database was compiled for samples collected from prominent eclogite and granulite occurrences. The $^{206}Pb/^{238}U$ dates for zircons of all samples show a large variability, and no single age can be calculated. The protolith ages remain unresolved due to the lack of coherent age groups at the upper end of the zircon age spectra. The spread in apparent ages is interpreted to be mainly caused by variable and possibly multi-stage Pb-loss. Further complexities are added by metamorphic zircon growth and re-equilibration processes, the unknown relevance of inherited components and possible mixing of different aged domains during analysis. A reliable interpretation of igneous crystallization ages is not yet possible. Previous studies and the new data document the importance of a Carboniferous metamorphic event at *c.* 340 Ma. The geological significance of this age group is controversial. Such ages have previously either been related to peak (U)HP conditions, the waning stages of eclogite-facies metamorphism or the amphibolite-facies overprint. This study provides new arguments for this discussion because, in both rock types, metamorphic zircon is characterized by very low total REE abundances, flat HREE patterns and the absence of an Eu anomaly. These features strongly suggest contemporaneous crystallization of zircon and garnet and strengthen interpretations proposing that the Carboniferous ages document late-stage eclogite-facies metamorphism, and not amphibolite-facies overprinting.

Keywords: eclogite, granulite, Orlica-Śnieżnik complex, zircon, U–Pb geochronology.

1. Introduction

Plausible geodynamic models of polymetamorphosed terranes require detailed knowledge of the magmatic and metamorphic processes that characterize the studied rock association. Crucial geochronological aspects are often poorly constrained and can only be revealed by application of a large number of different chronometric methods that specifically target different segments of the geological evolution. In spite of such efforts, the general picture may remain patchy, due to difficulties in linking age information to a distinct *P–T* stage, or because the last metamorphic overprint obscured traces of earlier events. This situation is encountered in the Orlica-Śnieżnik complex at the NE margin of the Bohemian Massif (Fig. 1a–c), where eclogites and granulites occur as isolated lenses within orthogneisses. Both rock types have attracted considerable attention due to (1) findings of presumed pseudomorphs after coesite and petrological considerations suggesting ultrahigh-pressure (UHP) metamorphic conditions (Bakun-Czubarow, 1991*a*,*b*, 1992; Bröcker & Klemd, 1996; Kryza, Pin & Vielzeuf, 1996; Klemd & Bröcker, 1999), and (2) favourable mineral assemblages that allow application of various geochronological methods (e.g. Brueckner, Medaris & Bakun-Czubarow, 1991; Lange *et al.* 2005*a*; Anczkiewicz *et al.* 2007; Bröcker *et al.* 2009). Understanding of the petrological and geochronological record of these rocks plays a key role in unravelling the geodynamic evolution of the eastern Variscides. Available concepts strongly depend on Sm–Nd, Ar–Ar, Rb–Sr and Lu–Hf dating. These methods allow easier linking of age information with specific *P–T–D* stages than does U–Pb zircon geochronology. On the other hand, U–Pb zircon dating is a more promising tool to unravel protolith ages and to reveal age information related to earlier metamorphic stages that is not disclosed by other dating methods with higher susceptibility to overprinting. Although some U–Pb

†Author for correspondence: brocker@uni-muenster.de

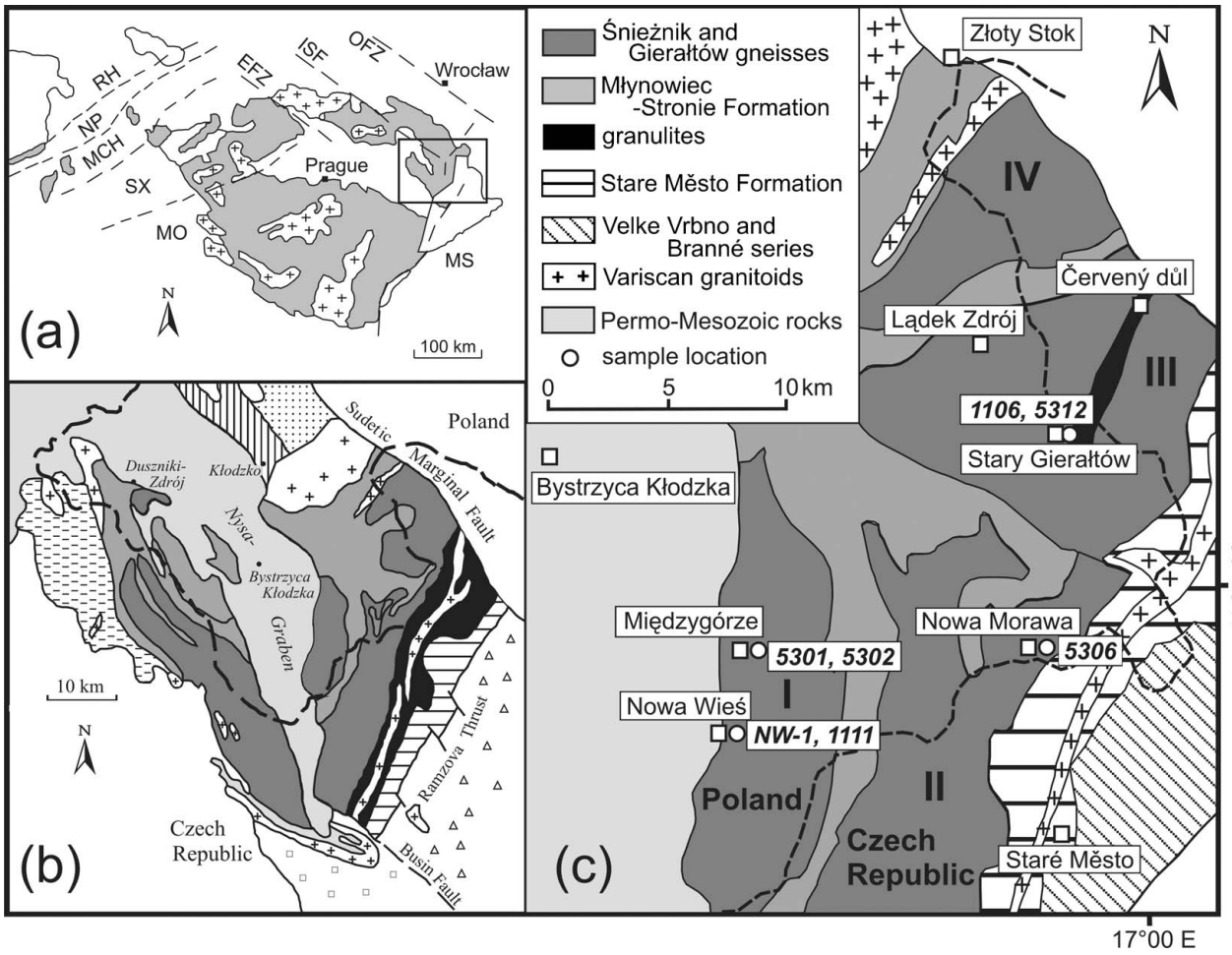

Figure 1. (a) Location of the Orlica-Śnieżnik complex within the Variscan belt. RH – Rhenohercynian Zone; NP – Northern Phyllite Zone; MCH – Mid-German Crystalline High; SX – Saxothuringian Zone; MO – Moldanubian Zone; OFZ – Odra Fault Zone; ISF – Intra-Sudetic Fault Zone; EFZ – Elbe Fault Zone; MS – Moravo-Silesian Zone. (b) Simplified geological map of the Orlica-Śnieżnik complex and neighbouring units (modified after Don *et al.* 1990; Turniak, Mazur & Wysoczanski, 2000). (c) Location of the study area in the eastern part of the Orlica-Śnieżnik complex (modified after Perchuk *et al.* 2005).

zircon data are available for the granulites (Klemd & Bröcker, 1999; Štípská, Schulmann & Kröner, 2004; Lange *et al.* 2005*a*; Anczkiewicz *et al.* 2007), a detailed and systematic U–Pb geochronological and zircon trace element study of the (U)HP rocks has not yet been carried out. The main aim of the present study is to assess the potential of zircon to obtain further insight into the geochronological history of these rocks. Using secondary ion mass spectrometry (SIMS) and laser ablation inductively coupled plasma mass spectrometry (LA-ICPMS), we have applied U–Pb zircon dating, trace element analysis and Ti-in-zircon thermometry to samples collected from some of the best preserved (U)HP occurrences of the Orlica-Śnieżnik complex.

2. Geological setting

The Orlica-Śnieżnik complex represents one of the major lithostratigraphic units of the West Sudetes and mainly consists of high-grade amphibolite-facies orthogneisses and schists (e.g. Don *et al.* 1990; Żelaźniewicz, Mazur & Szczepański, 2002). The orthogneisses have Cambrian protolith ages (*c.* 520–490 Ma; e.g. Oliver, Corfu & Krogh, 1993; Turniak, Mazur & Wysoczanski, 2000; Kröner *et al.* 2001; Štípská, Schulmann & Kröner, 2004) and record at least one episode of anatectic high-temperature (HT) metamorphism during Variscan time (e.g. Turniak, Mazur & Wysoczanski, 2000; Lange *et al.* 2002, 2005*b*; Bröcker *et al.* 2009), but possibly also migmatization in early Palaeozoic time (*c.* 515–485 Ma; Kröner *et al.* 2001; Żelaźniewicz *et al*. 2006). Comprehensive overviews of the geology of the Orlica-Śnieżnik complex were presented by Don *et al.* (1990), Żelaźniewicz, Mazur & Szczepański (2002) and Lange *et al.* (2005*b*). Here only a short summary of the features most relevant for the present study is given.

Eclogites locally occur as isolated blocks and lenses (up to tens of metres in size) within orthogneisses and are most common in a narrow NS-stretching zone (~ 3 km long) between the villages of Międzygórze and Nowa Wieś (e.g. Smulikowski, 1967; Bakun-Czubarow, 1968; Smulikowski & Smulikowski, 1985; Bröcker & Klemd, 1996; Don, 2001). Granulites are restricted to a NE-trending zone (up to 2 km wide and ~ 12 km long) in the eastern part of the study area

https://doi.org/10.1017/S0016756809990665 Published online by Cambridge University Press

(Fig. 1c; Pouba, Paděra & Fiala, 1985; Bakun-Czubarow, 1991*a*,*b*, 1992). Well-preserved outcrops are very rare. Several studies suggested that both eclogites and granulites have been tectonically incorporated into the orthogneisses (e.g. Don *et al.* 1990; Don, 2001). The most recent variants of such concepts propose that both rock types were transported to middle crustal levels by ductile vertical extrusion of a low viscosity matrix along relatively steep channels in front of a rigid backstop (e.g. Štípská, Schulmann & Kröner, 2004; Gordon *et al.* 2005; Schneider *et al*. 2006; Pressler *et al.* 2007). Other studies argued in favour of *in situ* (U)HP metamorphism (Brueckner, Medaris & Bakun-Czubarow, 1991; Bröcker & Klemd, 1996).

P–T estimates for eclogites suggest peak-pressures > 27 kbar at temperatures of 700–800 °C (e.g. Bakun-Czubarow, 1991*a*,*b*; Bröcker & Klemd, 1996). Significant differences in metamorphic conditions between discrete eclogite occurrences were not recognized. *P–T* estimates for granulites vary between ∼ 18 kbar and 900 °C (Štípská, Schulmann & Kröner, 2004) and 21–28 kbar at temperatures of 800–1000 °C (e.g. Bakun-Czubarow, 1991*a*,*b*, 1992; Kryza, Pin & Vielzeuf, 1996; Klemd & Bröcker, 1999). For the amphibolite-facies overprint, Klemd, Bröcker & Schramm (1995) reported pressure conditions of 4–11 kbar and temperatures of ∼ 600–650 °C. Microthermometric measurements on fluid inclusions suggest almost isothermal uplift from 7.5 kbar to about 2 kbar at 600 °C, followed by isobaric cooling to about 200 °C (Klemd, Bröcker & Schramm, 1995).

Protolith ages of the (U)HP rocks are only poorly constrained. A sensitive high-resolution ion microprobe (SHRIMP) U–Pb zircon age of *c.* 525 Ma for an eclogite was repeatedly quoted in the regional literature (e.g. Bakun-Czubarow, 1998, referring to D. Gebauer, unpub. data). Bakun-Czubarow (1991*b*) considered the granulites as derivatives of a Cadomian volcanic rock suite. For a felsic granulite, Štípská, Schulmann & Kröner (2004) reported a $^{206}Pb/^{238}U$ SHRIMP zircon age of 473 ± 8 Ma (1σ) for a single data point, interpreted to date an unspecified event in the history of the protolith. Based on U–Pb SHRIMP zircon dating of a mafic granulite, Lange *et al.* (2005*a*) suggested a minimum protolith age of *c.* 460 Ma.

Eclogites and granulites mostly yielded Variscan metamorphic ages (Sm–Nd, U–Pb, Ar–Ar, Rb–Sr) that range between 350 and 325 Ma (e.g. Brueckner, Medaris & Bakun-Czubarow, 1991; Steltenpohl *et al.* 1993; Klemd & Bröcker, 1999; Turniak, Mazur & Wysoczanski, 2000; Marheine *et al.* 2002; Lange *et al.* 2002, 2005*a*,*b*; Štípská, Schulmann & Kröner, 2004; Bröcker *et al.* 2009). Significant age differences between eclogites and granulites, and high temperature rocks recording amphibolite-facies overprinting, could not yet convincingly be resolved (e.g. Lange *et al.* 2005*a* and references therein). A prominent age cluster at *c.* 340 Ma has mostly been interpreted as a close approximation to peak (U)HP conditions (e.g. Brueckner, Medaris & Bakun-Czubarow, 1991; Štípská, Schulmann & Kröner, 2004; Lange *et al.* 2005*a*). In the case of the granulites, Anczkiewicz *et al.* (2007) concluded that the 340 Ma ages record amphibolite-facies overprinting. Based on a Lu–Hf garnet growth age and published zircon ages, these authors argued that the granulites experienced (U)HP metamorphism at some point between *c.* 387 and 360 Ma, but the exact timing of this metamorphic episode could not be further determined.

3. Sample description

Six samples were selected for zircon geochronology and seven samples for trace element studies from occurrences in and around Międzygórze, Nowa Wieś, Nowa Morawa and Stary Gierałtów (Fig. 1c). Eclogite samples from Międzygórze were collected from outcrops on the hilltop between the Wilczka and Bogoryja rivulets (5301), and on the western slope of Jawor Mountain (5302). Sample NW-1 represents an eclogite lens that is exposed about 1 km NE of Nowa Wieś (Bakun-Czubarow, 1968). Eclogite sample 1111 was taken from a loose block in the forest on the opposite side of the same valley. Eclogite 5306 is derived from the SE slope of Suszyca Mountain near Nowa Morawa. Sample 1106 was collected at Stary Gierałtów from the single outcrop of granulite on the Polish side of the border. Conventional ID-TIMS and ion-probe data for this sample have already been reported by Klemd & Bröcker (1999) and Lange *et al.* (2005*a*). Sample 5312 represents a loose block collected within the granulite belt, about 1.5 km ENE of Stary Gierałtów. GPS coordinates of the sample locations are reported in Tables 1 and 2, and in online Appendix Table A2 available at http://journals.cambridge.org/geo.

The common mineral assemblage of eclogites comprises garnet, clinopyroxene, zoisite, rutile and quartz. Varietal minerals include phengite, calcic amphibole and kyanite. Apatite, zircon and opaque phases are typical accessories. Retrograde phases include clinopyroxene(II), Ca-amphibole(II), biotite, epidote/clinozoisite, chlorite, albite, titanite and calcium carbonate. Sample 1106 is a mafic granulite mainly consisting of garnet, omphacite, plagioclase and quartz. Biotite and kyanite occur in small quantities. Typical accessories are rutile, apatite, zircon and Fe-oxides. The presence of pseudomorphs after coesite has been inferred from radial fractures around polycrystalline quartz inclusions in garnet (Klemd & Bröcker, 1999). Sample 5312 represents a granulite of intermediate bulk rock composition. The mineral assemblage is similar to 1106, but the modal proportions of garnet and omphacite are much lower, and kyanite has not been recognized. Additional phases, which are present in small quantities, are Ca-amphibole, titanite and K-feldspar. For field and petrological details of the eclogites and the granulites, see Smulikowski (1967), Smulikowski & Smulikowski (1985), Pouba, Paděra & Fiala (1985), Bakun-Czubarow (1991*a*,*b*, 1992),

https://doi.org/10.1017/S0016756809990665 Published online by Cambridge University Press

Table 1. SHRIMP U–Pb–Th analytical data for zircons from eclogite (5301, 5302) and granulite (5312)

Sample.spot	f^{206}Pb%	U ppm	Th ppm	^{232}Th/^{238}U	Rad. ^{206}Pb ppm	^{207}Pb/^{235} U	Error ±%	^{206}Pb/^{238}U	Error ±%	Rho	^{206}Pb–^{238}U age (Ma)	Error ± 1σ
5301.1.1	0.31	222	217	1.01	14.8	0.585	2.8	0.07741	1.4	0.500	480.7	6.6
5301.2.1	1.15	104	2	0.02	4.9	0.339	10.4	0.05399	1.7	0.166	339.0	5.7
5301.3.1	0.47	284	265	0.96	18.1	0.548	3.8	0.07387	1.4	0.376	459.4	6.4
5301.4.1	–	227	8	0.04	10.7	0.419	2.5	0.05499	1.5	0.574	345.1	4.9
5301.5.1	0.36	182	124	0.70	11.7	0.567	3.3	0.07436	1.5	0.442	462.4	6.5
5301.6.1	0.29	389	430	1.14	25.0	0.565	2.6	0.07460	1.4	0.533	463.8	6.3
5301.7.1	1.12	242	217	0.93	15.0	0.501	5.0	0.07105	1.4	0.288	442.5	6.2
5301.8.1	0.41	222	187	0.87	12.9	0.506	4.1	0.06753	1.5	0.357	421.3	5.9
5301.9.1	3.44	53	0	0.00	2.6	0.254	37.0	0.05525	2.4	0.065	346.7	8.2
5301.10.1	0.35	113	2	0.02	5.3	0.392	4.6	0.05497	1.7	0.359	345.0	5.5
5301.11.1	3.07	26	0	0.01	1.3	0.341	30.5	0.05658	2.8	0.093	354.8	9.8
5301.12.1	1.10	80	1	0.02	3.8	0.344	17.5	0.05486	2.0	0.113	344.3	6.6
5301.13.1	0.12	912	1393	1.58	59.7	0.585	1.8	0.07607	1.3	0.762	472.6	6.1
5302.1.1	0.11	644	907	1.45	41.1	0.580	3.8	0.07421	3.6	0.940	461.5	16.0
5302.2.1	–	184	160	0.90	12.3	0.630	4.6	0.07794	3.9	0.840	483.8	18.2
5302.3.1	–	198	217	1.13	13.1	0.615	4.1	0.07689	3.6	0.883	477.5	16.8
5302.4.1	0.01	167	154	0.95	10.3	0.575	4.2	0.07182	3.6	0.867	447.1	15.7
5302.5.1	0.25	138	96	0.72	8.4	0.549	4.6	0.07045	3.7	0.799	438.9	15.5
5302.6.1	0.78	105	103	1.01	6.7	0.540	7.8	0.07346	3.7	0.472	457.0	16.3
5302.7.1	0.15	285	173	0.63	18.8	0.595	4.1	0.07692	3.6	0.888	477.7	16.7
5302.8.1	0.14	108	83	0.79	6.5	0.549	4.9	0.07031	3.8	0.771	438.0	16.1
5302.9.1	–	279	3	0.01	12.9	0.420	4.8	0.05404	3.6	0.759	339.3	12.0
5302.10.1	0.21	168	3	0.02	8.2	0.407	4.6	0.05629	3.6	0.785	353.0	12.5
5302.10.2	0.79	281	344	1.26	17.3	0.544	5.5	0.07095	3.6	0.656	441.9	15.5
5312.1.1	0.07	377	256	0.70	23.5	0.563	1.8	0.07260	1.3	0.756	451.8	5.9
5312.1.2	0.34	65	97	1.55	3.0	0.387	6.5	0.05436	1.8	0.274	341.3	5.9
5312.2.1	–	197	84	0.44	11.1	0.518	2.7	0.06596	1.4	0.539	411.8	5.7
5312.3.1	0.83	170	65	0.39	7.9	0.350	6.9	0.05368	1.5	0.214	337.1	4.9
5312.4.1	0.02	494	160	0.33	24.2	0.424	1.8	0.05700	1.3	0.756	357.3	4.7
5312.5.1	0.34	354	140	0.41	19.5	0.465	3.3	0.06406	1.4	0.422	400.3	5.4
5312.5.2	0.93	152	260	1.78	6.9	0.338	7.2	0.05259	1.6	0.214	330.4	5.0
5312.6.1	0.50	128	65	0.52	8.7	0.599	3.9	0.07922	1.7	0.436	491.5	8.1
5312.7.1	0.35	308	122	0.41	20.5	0.592	2.6	0.07734	1.5	0.578	480.2	7.0
5312.8.1	–	257	68	0.27	13.8	0.478	2.2	0.06274	1.4	0.650	392.3	5.3
5312.9.1	–	199	59	0.31	11.1	0.514	2.6	0.06511	1.4	0.550	406.6	5.6
5312.10.1	0.26	300	92	0.32	16.3	0.464	3.5	0.06314	1.4	0.404	394.7	5.4
5312.11.1	–	413	144	0.36	20.8	0.448	2.2	0.05851	1.9	0.835	366.5	6.6
5312.12.1	0.55	264	127	0.50	14.6	0.451	3.8	0.06398	1.4	0.376	399.8	5.5

f^{206}Pb% indicates the percentage of ^{206}Pb that is common Pb; Rad. ^{206}Pb = radiogenic ^{206}Pb. Uncertainties are reported at the 1σ level. Common Pb corrected using measured ^{204}Pb. Error in standard calibration was 0.41% (samples 5301, 5312) and 0.59% (sample 5302), respectively.
Sample locations: 5301 = Międzygórze, N 50°13.798′, E 016°46.142′ ; 5302 = Międzygórze, N 50°13.548′, E 016°46.097′; 5312 = Stary Gierałtów, N 50°18.545′, E 016°57.472′.

Dumicz (1993), Kryza, Pin & Vielzeuf (1996), Bröcker & Klemd (1996), Klemd & Bröcker (1999) and Perchuk *et al.* (2005).

4. Analytical methods

All eclogites and granulites record indications for amphibolite-facies overprinting. Sample selection was guided by the attempt to collect the most pristine parts of individual occurrences. For U–Pb geochronology and trace element studies, zircon was separated from ~ 1.5–12 kg samples by standard routines (jawbreaker, disc mill, Wilfley table, Frantz magnetic separator, heavy liquids). After polishing to expose the grain interior, CL imaging was applied to reveal the internal zircon structures and to guide spot placement. SIMS U–Pb dating was carried out by use of a sensitive high-resolution ion microprobe (SHRIMP) at the Centre of Isotopic Research (VSEGEI), St Petersburg, Russia. Handpicked zircon grains were mounted in 25 mm epoxy discs together with pieces of the Temora-1 (Black *et al.* 2003) and 91500 zircon standards (Wiedenbeck *et al.* 1995; U = 81.2 ppm). Including both spike-calibration and U decay constant uncertainties, the total uncertainty of the Temora-1 standard is 416.8 ± 1.3 Ma, and a value of 417 Ma was used for age calculation in this study. Analytical procedures followed standard operating routines and were similar to those reported by Williams (1998) and Larionov, Andreichev & Gee (2004). Cleaned zircon mounts were gold-coated and analysed for U–Th–Pb isotopes using a primary beam diameter of ~ 20 μm. Before analysis, the primary beam was rastered over the target area for ~ 30 s. The data were collected in sets of five scans through $^{196}Zr_2O$, ^{204}Pb, background (~ 204.5), ^{206}Pb, ^{207}Pb, ^{208}Pb, ^{238}U, ^{248}ThO and ^{254}UO. The Temora standard was analysed after every fifth unknown. The data were reduced using the SQUID v. 1.12 Excel Macro of Ludwig (2005*a*). Uncertainties given for individual SHRIMP data points (ratios and

https://doi.org/10.1017/S0016756809990665 Published online by Cambridge University Press

Table 2. LA-ICPMS U-Pb data for (U)HP rocks of the Orlica-Śnieżnik complex

		Isotopic ratios									Ages (Ma)					
Spot	CL type	$^{206}Pb/^{204}Pb$	*f* 206%	$^{206}Pb/^{238}U$	±2σ	$^{207}Pb/^{235}U$	±2σ	$^{207}Pb/^{206}Pb$	±2σ	rho	$^{206}Pb–^{238}U$	±2σ	$^{207}Pb–^{235}U$	±2σ	$^{207}Pb–^{206}Pb$	±2σ
Eclogite 5301; sample location: Międzygórze, N 50° 13.798′, E 016° 46.142′																
5301B_1	2	11504	0.06	0.06741	0.00208	0.56344	0.05169	0.06062	0.00524	0.34	420.5	12.6	453.8	33.6	625.9	187.0
5301B_2	2	1085	1.43	0.05948	0.00167	0.47447	0.02481	0.05786	0.00255	0.54	372.4	10.1	394.3	17.1	524.5	96.9
5301B_3	2	–	–	0.05239	0.00121	0.39729	0.01567	0.05500	0.00176	0.58	329.2	7.4	339.7	11.4	412.4	71.6
5301B_4	2	–	–	0.05713	0.00123	0.43585	0.01758	0.05533	0.00189	0.54	358.1	7.5	367.3	12.4	425.7	76.0
5301B_5	2	18930	0.09	0.06086	0.00116	0.45619	0.01259	0.05436	0.00109	0.69	380.9	7.0	381.6	8.8	386.2	44.9
5301B_6	2	5101	0.23	0.06152	0.00152	0.46824	0.02443	0.05520	0.00254	0.47	384.8	9.2	390.0	16.9	420.6	102.7
5301B_7	2	–	–	0.05820	0.00195	0.45809	0.02824	0.05709	0.00296	0.54	364.7	11.8	382.9	19.7	495.0	114.3
5301B_9	2	3178	0.52	0.05804	0.00129	0.43947	0.01422	0.05492	0.00129	0.69	363.7	7.9	369.9	10.0	408.9	52.5
5301B_10	2	153	10.28	0.05419	0.00240	0.39375	0.02347	0.05270	0.00210	0.74	340.2	14.7	337.1	17.1	316.1	90.9
5301B_11	2	–	–	0.06014	0.00162	0.45154	0.01934	0.05445	0.00181	0.63	376.5	9.9	378.4	13.5	389.8	74.7
5301B_12	2	–	–	0.06828	0.00231	0.52724	0.02781	0.05601	0.00227	0.64	425.8	13.9	430.0	18.5	452.7	90.1
5301B_13	2	8441	0.14	0.05520	0.00206	0.40530	0.01775	0.05325	0.00123	0.85	346.3	12.6	345.5	12.8	339.7	52.2
5301_14	2	215	5.04	0.05761	0.00158	0.42436	0.01709	0.05342	0.00157	0.68	361.1	9.6	359.2	12.2	346.9	66.6
5301_15	2	–	–	0.05616	0.00310	0.40729	0.03102	0.05260	0.00277	0.72	352.2	18.9	346.9	22.4	311.7	119.9
5301_16	2	2671	0.46	0.06078	0.00158	0.45287	0.01631	0.05404	0.00135	0.72	380.4	9.6	379.3	11.4	372.6	56.3
5301_17	2	1344	0.62	0.05968	0.00155	0.44767	0.01855	0.05441	0.00175	0.63	373.7	9.4	375.6	13.0	387.9	72.4
5301_19	2	–	–	0.05281	0.00130	0.38769	0.01712	0.05324	0.00195	0.56	331.7	8.0	332.7	12.5	339.3	83.0
5301_20	2	–	–	0.05316	0.00090	0.39009	0.01304	0.05322	0.00153	0.50	333.9	5.5	334.4	9.5	338.2	65.4
5301_P1	1	2127	0.83	0.08872	0.00160	0.71209	0.02210	0.05821	0.00147	0.58	548.0	9.5	546.0	13.1	537.7	55.3
5301_P2	1	22934	0.08	0.07642	0.00231	0.59435	0.02359	0.05641	0.00145	0.76	474.7	13.8	473.6	15.0	468.5	57.1
5301_P3	1	16384	0.11	0.08686	0.00216	0.69568	0.02286	0.05809	0.00125	0.76	536.9	12.8	536.2	13.7	533.2	47.1
5301_P4	1	2502	0.72	0.07765	0.00154	0.60469	0.01999	0.05648	0.00149	0.60	482.0	9.2	480.2	12.6	471.4	58.6
5301_P5	1	14705	0.12	0.08355	0.00136	0.66697	0.01779	0.05789	0.00123	0.61	517.3	8.1	518.9	10.8	525.9	46.4
5301_P6	1	3727	0.35	0.08339	0.00135	0.65745	0.01747	0.05718	0.00120	0.61	516.3	8.0	513.1	10.7	498.5	46.4
5301_P7	1	21319	0.08	0.08307	0.00148	0.66075	0.01819	0.05769	0.00121	0.65	514.4	8.8	515.1	11.1	518.1	46.0
5301_P8	1	3959	0.41	0.08973	0.00149	0.72172	0.01752	0.05833	0.00103	0.68	553.9	8.8	551.7	10.3	542.4	38.8
5301_P9	1	5666	0.32	0.07835	0.00165	0.63206	0.02115	0.05851	0.00152	0.63	486.3	9.8	497.4	13.2	548.8	56.9
5301_P10	1	13507	0.12	0.08134	0.00123	0.64423	0.01210	0.05744	0.00064	0.81	504.1	7.3	504.9	7.5	508.7	24.5
5301_P11	1	4857	0.37	0.08355	0.00167	0.66165	0.01677	0.05744	0.00089	0.79	517.2	10.0	515.6	10.2	508.5	34.1
5301_P12	1	3239	0.53	0.08052	0.00182	0.63500	0.01832	0.05720	0.00103	0.78	499.2	10.9	499.2	11.4	499.3	39.5
5301_P13	1	2919	0.62	0.07492	0.00291	0.59359	0.02597	0.05746	0.00116	0.89	465.7	17.5	473.2	16.5	509.3	44.3
5301_P14	1	4590	0.39	0.09021	0.00209	0.73292	0.02220	0.05893	0.00115	0.76	556.8	12.3	558.3	13.0	564.4	42.6
5301_P15	1	7242	0.24	0.07546	0.00227	0.58872	0.02022	0.05658	0.00093	0.88	469.0	13.6	470.0	12.9	475.3	36.5
5301_P16	1	10219	0.17	0.08070	0.00224	0.65583	0.02344	0.05894	0.00133	0.78	500.3	13.4	512.1	14.4	565.1	49.0
5301_P17	1	13452	0.13	0.08109	0.00207	0.63659	0.01853	0.05694	0.00080	0.88	502.6	12.3	500.2	11.5	489.2	31.0
5301_P18	1	–	–	0.08039	0.00251	0.63187	0.02157	0.05701	0.00078	0.92	498.4	15.0	497.3	13.4	491.9	30.4
5301_P19	1	2571	0.70	0.07896	0.00174	0.61994	0.01978	0.05694	0.00131	0.69	489.9	10.4	489.8	12.4	489.4	50.9
5301_P20	1	36761	0.04	0.08184	0.00210	0.64567	0.01814	0.05722	0.00065	0.92	507.1	12.5	505.8	11.2	499.9	24.9
5301_P21	1	2850	0.63	0.06329	0.00160	0.47775	0.01300	0.05474	0.00055	0.93	395.6	9.7	396.5	8.9	401.9	22.4
5301_P22	1	1203071	0.00	0.08246	0.00202	0.65054	0.01731	0.05722	0.00060	0.92	510.8	12.0	508.8	10.6	500.0	23.0
5301B_P23	1	2577	0.70	0.07094	0.00341	0.54744	0.02929	0.05597	0.00131	0.90	441.8	20.5	443.3	19.2	451.1	52.0
5301B_P24	1	1324	1.36	0.06356	0.00286	0.47634	0.02974	0.05436	0.00235	0.72	397.2	17.3	395.6	20.5	385.9	97.3
5301B_P25	1	9861	0.18	0.08482	0.00223	0.68065	0.01990	0.05820	0.00074	0.90	524.8	13.3	527.2	12.0	537.3	27.9
5301B_P26	1	4325	0.41	0.09731	0.00125	0.80614	0.01578	0.06008	0.00089	0.66	598.6	7.3	600.3	8.9	606.7	32.0
5301B_P27	1	57516	0.02	0.07404	0.00202	0.57679	0.01719	0.05650	0.00067	0.92	460.5	12.1	462.4	11.1	472.0	26.4
5301B_P28	1	2471	0.73	0.06170	0.00171	0.46655	0.01809	0.05484	0.00149	0.71	385.9	10.4	388.8	12.5	405.8	60.8

Table 2. (*Cont.*)

Spot	CL type	Isotopic ratios									Ages (Ma)					
		$^{206}Pb/^{204}Pb$	*f* 206%	$^{206}Pb/^{238}U$	±2σ	$^{207}Pb/^{235}U$	±2σ	$^{207}Pb/^{206}Pb$	±2σ	rho	$^{206}Pb–^{238}U$	±2σ	$^{207}Pb–^{235}U$	±2σ	$^{207}Pb–^{206}Pb$	±2σ
5301B_P29	1	14217	0.12	0.08185	0.00108	0.64530	0.01082	0.05718	0.00059	0.79	507.1	6.5	505.6	6.7	498.6	22.7
5301B_P30	1	25245	0.07	0.07939	0.00113	0.62095	0.01115	0.05673	0.00062	0.79	492.4	6.8	490.4	7.0	481.2	24.1
5301B_P31	1	–	–	0.07706	0.00233	0.60428	0.02044	0.05687	0.00087	0.89	478.6	13.9	479.9	12.9	486.6	33.7
5301B_P32	3	11427	0.16	0.05291	0.00170	0.39123	0.01439	0.05363	0.00096	0.87	332.3	10.4	335.3	10.5	355.6	40.2
5301B_P33	1	4513	0.39	0.08482	0.00257	0.69551	0.02399	0.05947	0.00098	0.88	524.8	15.2	536.1	14.4	584.3	35.9
5301B_P34	1	15307	0.09	0.08624	0.00268	0.68115	0.02472	0.05729	0.00107	0.86	533.2	15.9	527.5	14.9	502.6	41.3
5301B_P35	1	6307	0.28	0.08663	0.00269	0.71116	0.02480	0.05954	0.00095	0.89	535.6	15.9	545.4	14.7	586.9	34.7
5301B_P36	1	19480	0.09	0.08328	0.00278	0.65637	0.02378	0.05716	0.00081	0.92	515.7	16.5	512.4	14.6	497.8	31.1
5301B_P37	1	10482	0.15	0.07538	0.00218	0.58783	0.01865	0.05656	0.00075	0.91	468.5	13.0	469.5	11.9	474.5	29.2
5301B_P38	1	5186	0.34	0.07887	0.00261	0.63997	0.02339	0.05885	0.00092	0.90	489.4	15.6	502.3	14.5	561.5	34.1
5301B_P39	1	6118	0.29	0.08642	0.00271	0.69318	0.02337	0.05818	0.00072	0.93	534.3	16.1	534.7	14.0	536.5	27.1
5301B_P40	1	9825	0.12	0.07816	0.00183	0.61245	0.01678	0.05683	0.00081	0.85	485.1	10.9	485.1	10.6	484.9	31.6
5301B_P41	1	5044	0.35	0.08876	0.00191	0.72021	0.02021	0.05885	0.00106	0.77	548.2	11.3	550.8	11.9	561.6	39.3
5301B_P42	1	2987	0.59	0.09214	0.00218	0.75404	0.02283	0.05935	0.00112	0.78	568.2	12.9	570.6	13.2	580.2	41.1
5301B_P45	1	1985	0.64	0.08171	0.00137	0.64271	0.01405	0.05705	0.00080	0.77	506.3	8.1	504.0	8.7	493.5	31.0
5301B_P46	1	2560	0.70	0.07206	0.00158	0.55258	0.01685	0.05562	0.00118	0.72	448.5	9.5	446.7	11.0	437.2	47.2
5301B_P47	1	13929	0.11	0.08533	0.00201	0.68194	0.01841	0.05796	0.00077	0.87	527.9	11.9	527.9	11.1	528.3	28.9
5301B_P44	1	15442	0.10	0.08466	0.00159	0.67924	0.01600	0.05819	0.00083	0.80	523.8	9.5	526.3	9.7	537.1	31.0
5301B_P49	1	3943	0.45	0.09471	0.00171	0.78673	0.01739	0.06025	0.00077	0.82	583.3	10.1	589.3	9.9	612.5	27.7
Granulite 5312; sample location: Stary Gieraltów, N 50° 18.545′, E 016° 57.472′																
5312_1	2	–	–	0.05203	0.00110	0.38124	0.01594	0.05314	0.00192	0.50	327.0	6.7	328.0	11.7	334.9	81.9
5312_2	1	–	–	0.06805	0.00144	0.51667	0.01393	0.05507	0.00092	0.79	424.4	8.7	422.9	9.3	415.1	37.3
5312_3	1	–	–	0.06171	0.00103	0.46444	0.01141	0.05458	0.00098	0.68	386.0	6.3	387.3	7.9	395.3	40.4
5312_4	3	–	–	0.05306	0.00099	0.38761	0.00936	0.05298	0.00081	0.78	333.3	6.1	332.6	6.9	327.9	34.6
5312_5	3	194541	0.01	0.05512	0.00179	0.40548	0.01493	0.05335	0.00093	0.88	345.9	10.9	345.6	10.8	344.0	39.2
5312_6	1	2712	0.48	0.06716	0.00210	0.51060	0.01865	0.05514	0.00104	0.86	419.0	12.7	418.9	12.5	418.0	42.1
5312_7	1	18834	0.09	0.07859	0.00310	0.61714	0.02666	0.05695	0.00101	0.91	487.7	18.5	488.1	16.7	489.7	39.0
5312_8	2	70736	0.01	0.05809	0.00179	0.43140	0.01727	0.05386	0.00137	0.77	364.0	10.9	364.2	12.3	365.3	57.6
5312_9	1	–	–	0.07283	0.00205	0.56268	0.01907	0.05603	0.00106	0.83	453.2	12.3	453.3	12.4	453.8	42.0
5312_10	2	–	–	0.06134	0.00251	0.45826	0.02039	0.05418	0.00094	0.92	383.8	15.3	383.0	14.2	378.7	38.9
5312_11	2	67318	0.02	0.05820	0.00218	0.43290	0.01800	0.05395	0.00098	0.90	364.6	13.3	365.2	12.8	369.0	40.9
5312_12	3	33795	0.03	0.05741	0.00215	0.42359	0.01799	0.05352	0.00107	0.88	359.8	13.1	358.6	12.8	350.8	45.1
5312_13	3	–	–	0.05572	0.00196	0.41272	0.01617	0.05372	0.00093	0.90	349.5	11.9	350.8	11.6	359.3	39.2
5312_14	3	14658	0.12	0.05305	0.00229	0.38821	0.01850	0.05308	0.00108	0.90	333.2	14.0	333.1	13.5	332.2	46.3
5312_15	1	71469	0.01	0.06399	0.00166	0.49842	0.01755	0.05650	0.00134	0.74	399.8	10.1	410.6	11.9	472.0	52.7
5312_16	3	17529	0.07	0.05736	0.00148	0.42368	0.01407	0.05357	0.00112	0.78	359.5	9.0	358.7	10.0	353.1	47.2
5312_17	2	464255	0.00	0.05789	0.00144	0.42903	0.01592	0.05375	0.00148	0.67	362.7	8.8	362.5	11.3	360.8	62.2
5312_18	1	7293	0.22	0.08706	0.00229	0.70049	0.02609	0.05835	0.00154	0.71	538.1	13.6	539.1	15.6	543.2	57.7
5312_19	1	–	–	0.07179	0.00224	0.55378	0.02229	0.05595	0.00143	0.77	446.9	13.4	447.5	14.6	450.3	56.7
5312_20	3	74508	0.02	0.05339	0.00226	0.38807	0.01891	0.05272	0.00127	0.87	335.3	13.9	333.0	13.8	316.9	54.6
5312_21	2	–	–	0.06097	0.00228	0.45627	0.02226	0.05427	0.00170	0.77	381.5	13.9	381.7	15.5	382.5	70.4
5312_22	1	221226	0.01	0.07688	0.00268	0.60120	0.02393	0.05671	0.00109	0.87	477.5	16.0	478.0	15.2	480.5	42.6
5312_23	1	34410	0.04	0.05631	0.00195	0.41498	0.01679	0.05345	0.00112	0.86	353.2	11.9	352.5	12.0	347.8	47.3
5312_24	3	71564	0.02	0.05396	0.00190	0.39363	0.01432	0.05291	0.00049	0.97	338.8	11.6	337.0	10.4	324.8	21.0
5312_25	1	–	–	0.07524	0.00255	0.59256	0.02163	0.05712	0.00078	0.93	467.7	15.3	472.5	13.8	496.1	29.9
5312_26	3	23246	0.06	0.05478	0.00180	0.40083	0.01383	0.05306	0.00055	0.95	343.8	11.0	342.2	10.0	331.6	23.3

Table 2. (*Cont.*)

Spot	CL type	Isotopic ratios									Ages (Ma)					
		$^{206}Pb/^{204}Pb$	f 206%	$^{206}Pb/^{238}U$	±2σ	$^{207}Pb/^{235}U$	±2σ	$^{207}Pb/^{206}Pb$	±2σ	rho	$^{206}Pb–^{238}U$	±2σ	$^{207}Pb–^{235}U$	±2σ	$^{207}Pb–^{206}Pb$	±2σ
5312_27	3	168749	0.01	0.04863	0.00180	0.35975	0.01411	0.05365	0.00069	0.94	306.1	11.1	312.0	10.5	356.5	29.1
5312_28	3	10352	0.07	0.05488	0.00190	0.40158	0.01462	0.05307	0.00061	0.95	344.4	11.6	342.8	10.6	331.8	26.1
5312_29	3	–	–	0.06721	0.00211	0.51699	0.01825	0.05579	0.00090	0.89	419.3	12.7	423.1	12.2	444.1	35.9
5312_30	1	42371	0.04	0.07544	0.00188	0.58468	0.01732	0.05621	0.00089	0.84	468.8	11.3	467.5	11.1	460.8	35.3
5312_31	3	126660	0.01	0.05137	0.00131	0.37468	0.01073	0.05290	0.00069	0.89	322.9	8.0	323.1	7.9	324.4	29.6
5312_32	2	198650	0.01	0.05317	0.00166	0.39401	0.01447	0.05375	0.00104	0.85	333.9	10.2	337.3	10.5	360.6	43.5
5312_33	3	66174	0.02	0.05296	0.00135	0.38824	0.01096	0.05317	0.00065	0.90	332.7	8.3	333.1	8.0	336.1	27.7
5312_34	1	–	–	0.07116	0.00237	0.54881	0.01986	0.05593	0.00078	0.92	443.1	14.3	444.2	13.0	449.8	31.1
5312_35	3	71443	0.02	0.05490	0.00163	0.40598	0.01307	0.05364	0.00066	0.92	344.5	10.0	346.0	9.4	355.8	27.9
5312_36	2	7669	0.23	0.05781	0.00225	0.42938	0.01886	0.05387	0.00109	0.89	362.3	13.7	362.7	13.4	365.7	45.7
5312_37	1	–	–	0.07263	0.00242	0.56338	0.02167	0.05626	0.00108	0.87	452.0	14.5	453.7	14.1	462.6	42.6
5312_37	2	12973	0.11	0.06380	0.00265	0.48145	0.02208	0.05473	0.00106	0.91	398.7	16.1	399.1	15.1	401.2	43.4
5312_38	2	589225	0.00	0.05525	0.00283	0.40395	0.02292	0.05303	0.00130	0.90	346.7	17.3	344.5	16.6	330.0	55.7
5312_39	1	11382	0.16	0.06671	0.00331	0.50506	0.02878	0.05491	0.00154	0.87	416.3	20.0	415.1	19.4	408.7	62.8
5312_40	2	1240	0.58	0.04800	0.00194	0.34338	0.01603	0.05189	0.00121	0.87	302.2	11.9	299.7	12.1	280.6	53.5
5312_41	3	42368	0.02	0.05486	0.00147	0.40334	0.01389	0.05333	0.00115	0.78	344.3	9.0	344.1	10.0	342.8	48.8
5312_42	3	8122	0.16	0.04661	0.00160	0.33560	0.01298	0.05222	0.00093	0.89	293.7	9.9	293.8	9.9	295.1	40.6
5312_43	2	13623	0.11	0.06446	0.00196	0.48703	0.01850	0.05480	0.00124	0.80	402.7	11.9	402.9	12.6	404.1	50.8
5312_44	3	–	–	0.05163	0.00136	0.37578	0.01157	0.05278	0.00084	0.86	324.5	8.3	323.9	8.5	319.6	36.2
5312_45	2	37819	0.03	0.06000	0.00121	0.44950	0.01256	0.05434	0.00105	0.72	375.6	7.3	376.9	8.8	385.1	43.6
5312_46	1	34309	0.04	0.07637	0.00153	0.59554	0.01590	0.05656	0.00100	0.75	474.4	9.1	474.4	10.1	474.4	39.2
5312_47	1	15875	0.07	0.07431	0.00188	0.57518	0.01799	0.05614	0.00103	0.81	462.0	11.3	461.4	11.6	458.0	40.7
5312_48	2	7769	0.19	0.06429	0.00192	0.48107	0.01751	0.05427	0.00113	0.82	401.7	11.6	398.8	12.0	382.2	47.0
5312_49	1	–	–	0.06856	0.00115	0.52332	0.01239	0.05536	0.00092	0.71	427.4	7.0	427.4	8.3	426.9	37.2
5312_50	1	22050	0.05	0.06870	0.00134	0.52708	0.01447	0.05564	0.00108	0.71	428.3	8.1	429.9	9.6	438.2	43.1
5312_51	1	19106	0.07	0.05961	0.00138	0.44441	0.01288	0.05408	0.00095	0.80	373.2	8.4	373.4	9.1	374.3	39.4
5312_52	2	3001	0.51	0.05286	0.00122	0.38583	0.01075	0.05294	0.00083	0.83	332.0	7.5	331.3	7.9	326.3	35.5
5312_53	1	–	–	0.07103	0.00147	0.54616	0.01420	0.05576	0.00088	0.80	442.4	8.8	442.5	9.3	443.1	35.0
5312_54	1	6124	0.29	0.08119	0.00245	0.63896	0.02177	0.05708	0.00091	0.88	503.2	14.6	501.7	13.5	494.6	35.1
5312_55	2	–	–	0.05436	0.00158	0.39792	0.01591	0.05309	0.00145	0.73	341.2	9.7	340.1	11.6	332.6	62.1
5312_56	3	312426	0.00	0.05647	0.00211	0.41643	0.01603	0.05349	0.00051	0.97	354.1	12.9	353.5	11.5	349.6	21.4
5312_57	1	–	–	0.06731	0.00259	0.51503	0.02105	0.05549	0.00076	0.94	419.9	15.7	421.8	14.1	432.3	30.6
5312_58	1	–	–	0.07709	0.00320	0.60267	0.02614	0.05670	0.00073	0.96	478.7	19.1	478.9	16.6	479.8	28.3
5312_59	2	4060390	0.00	0.05813	0.00222	0.43126	0.01770	0.05381	0.00080	0.93	364.2	13.6	364.1	12.6	363.2	33.4
5312_60	3	151972	0.01	0.05038	0.00235	0.36452	0.01770	0.05248	0.00072	0.96	316.8	14.4	315.6	13.2	306.5	31.4
5312_61	1	–	–	0.07473	0.00318	0.57987	0.02602	0.05628	0.00080	0.95	464.6	19.1	464.4	16.7	463.4	31.6
5312_62	3	144938	0.01	0.05206	0.00247	0.38010	0.01898	0.05295	0.00082	0.95	327.2	15.1	327.1	14.0	326.8	35.2
5312_63	3	4582609	0.00	0.05122	0.00238	0.37269	0.01813	0.05277	0.00078	0.95	322.0	14.6	321.6	13.4	318.9	33.5

Table 2. (*Cont.*)

Spot	CL type	Isotopic ratios									Ages					
		$^{206}Pb/^{204}Pb$	$f206\%$	$^{206}Pb/^{238}U$	$\pm2\sigma$	$^{207}Pb/^{235}U$	$\pm2\sigma$	$^{207}Pb/^{206}Pb$	$\pm2\sigma$	rho	$^{206}Pb–^{238}U$	$\pm2\sigma$	$^{207}Pb–^{235}U$	$\pm2\sigma$	$^{207}Pb–^{206}Pb$	$\pm2\sigma$
5312_64	1	42728	0.04	0.06560	0.00281	0.50267	0.02269	0.05558	0.00080	0.95	409.6	17.0	413.5	15.3	435.6	32.0
5312_65	3	67477	0.02	0.05023	0.00217	0.36441	0.01720	0.05262	0.00100	0.92	315.9	13.3	315.5	12.8	312.3	43.2
5312_66	1	58053	0.02	0.07075	0.00297	0.54546	0.02445	0.05591	0.00089	0.94	440.7	17.9	442.0	16.1	449.1	35.3
5312_67	1	35267	0.04	0.06491	0.00268	0.49072	0.02161	0.05483	0.00085	0.94	405.4	16.2	405.4	14.7	405.6	34.6
5312_68	2	4006	0.38	0.05261	0.00254	0.38480	0.02052	0.05305	0.00119	0.91	330.5	15.6	330.6	15.0	331.0	51.0
5312_69	3	–	–	0.04893	0.00218	0.35301	0.01671	0.05232	0.00084	0.94	307.9	13.4	307.0	12.5	299.7	36.7
5312_70	3	64755	0.02	0.04633	0.00142	0.33307	0.01086	0.05214	0.00057	0.94	291.9	8.8	291.9	8.3	291.6	24.9
5312_71	3	49489	0.02	0.06639	0.00223	0.50499	0.01921	0.05517	0.00098	0.88	414.4	13.5	415.1	13.0	419.0	39.7
5312_72	2	17675	0.07	0.05219	0.00186	0.38246	0.01560	0.05315	0.00106	0.87	327.9	11.4	328.8	11.5	335.4	45.2
5312_73	3	42672	0.03	0.05049	0.00164	0.36921	0.01318	0.05304	0.00078	0.91	317.5	10.1	319.1	9.8	330.6	33.2
5312_73A	1	216433	0.01	0.06908	0.00216	0.53282	0.01849	0.05594	0.00085	0.90	430.6	13.0	433.7	12.2	450.3	33.7
5312_74	3	–	–	0.05140	0.00151	0.37502	0.01182	0.05291	0.00060	0.93	323.1	9.3	323.4	8.7	325.2	25.7
5312_75	2	17727	0.10	0.05981	0.00196	0.44790	0.01738	0.05431	0.00113	0.84	374.5	11.9	375.8	12.2	383.9	46.8
5312_76	2	–	–	0.05418	0.00180	0.40553	0.01565	0.05428	0.00107	0.86	340.1	11.0	345.6	11.3	382.9	44.1
5312_77	1	208533	0.01	0.06469	0.00190	0.50183	0.01629	0.05627	0.00078	0.90	404.1	11.5	412.9	11.0	462.9	30.9
5312_78	1	24908	0.06	0.06657	0.00165	0.52495	0.01751	0.05719	0.00127	0.75	415.5	10.0	428.5	11.7	498.9	49.0
5312_79	3	35927	0.04	0.05229	0.00137	0.38128	0.01266	0.05288	0.00108	0.79	328.6	8.4	328.0	9.3	323.8	46.5
5312_80	1	26978	0.05	0.06697	0.00172	0.50932	0.01650	0.05516	0.00109	0.79	417.8	10.4	418.0	11.1	418.9	44.3
5312_81	1	21362	0.04	0.07111	0.00178	0.54906	0.01865	0.05600	0.00129	0.74	442.8	10.7	444.4	12.2	452.3	51.0
5312_82	3	81954	0.02	0.05650	0.00145	0.41726	0.01389	0.05356	0.00114	0.77	354.3	8.8	354.1	10.0	352.8	48.1
5312_83	3	126632	0.01	0.05783	0.00205	0.42935	0.01756	0.05385	0.00110	0.87	362.4	12.5	362.7	12.5	364.8	46.1
5312_84	2	7356	0.16	0.06138	0.00219	0.46146	0.01978	0.05453	0.00130	0.83	384.0	13.3	385.3	13.7	393.0	53.3
5312_85	3	23947	0.07	0.05611	0.00217	0.41042	0.01764	0.05305	0.00099	0.90	351.9	13.3	349.2	12.7	331.0	42.2
5312_86	1	17190	0.06	0.07228	0.00270	0.55682	0.02420	0.05587	0.00124	0.86	449.9	16.3	449.5	15.8	447.3	49.2

All uncertainties are absolute values (2σ); – indicates ^{204}Pb below detection limit.

ages) are reported at the 1σ level; error ellipses are shown with 2σ uncertainty. In the text, individual ages and weighted averages are quoted as ^{206}Pb–^{238}U ages with 2σ uncertainty. Common Pb corrections were performed using the relevant Pb composition after Stacey & Kramers (1975) and measured ^{204}Pb (Compston, Williams & Meyer, 1984). Most analyses contain very little common Pb and thus are insensitive to the choice of initial isotope composition.

For LA-ICPMS geochronological studies, new sample mounts were prepared, because only a relatively small number of grains were available on the SHRIMP epoxy discs. These age determinations and the trace element analyses were performed on a sector field ICP-MS (Element2, ThermoFinnigan) coupled to a 193 nm ArF Excimer laser system (UP193HE, New Wave Research) at the Institut für Mineralogie, Universität Münster. The instrument parameters for both the laser and the ICP-MS are listed in Table A1 (http://journals.cambridge.org/geo). For U–Pb analysis the masses 202, 204, 206, 207 and 238 were measured. ^{202}Hg was also analysed to quantify the interference of ^{204}Hg on ^{204}Pb. Corrections for laser-induced elemental fractionation and instrumental mass bias were done by bracketing groups of five unknowns with two measurements of the GJ-1 standard zircon (Jackson *et al.* 2004). Age calculations were done offline with an in-house Excel spreadsheet. Corrections were applied for gas blank, time-dependent elemental fractionation (Sylvester & Ghaderi, 1997) and common Pb, if present. A common Pb correction (Stacey & Kramers, 1975) was only applied if the contribution of the common ^{206}Pb to the total measured ^{206}Pb was 0.7 % or higher. Analyses that showed in-run ^{204}Pb anomalies but 'normal' average ^{204}Pb values were subjected to a common Pb correction applied to the anomalous ratios only. Uncertainties given for individual LA-ICPMS U–Pb zircon analyses (ratios, ages, error ellipses) are reported with 2σ uncertainty. To monitor reproducibility of the ^{206}Pb–^{238}U ages, the Plešovice standard zircon (337.3 ± 0.4 Ma; Sláma *et al.* 2008) was analysed and processed as an unknown. The results of 30 spot analyses are shown in Figure 2. The plots, regressions and weighted mean age calculations were carried out using Isoplot/Ex 3.22 (Ludwig, 2005*b*). Decay constants used for SHRIMP and LA-ICPMS age calculations are those recommended by the Subcommission on Geochronology of IUGS (Steiger & Jäger, 1977).

For trace element analysis of samples 5301, 5302, 5306 and 5312, available SHRIMP mounts were used, and spot selection was guided by the U–Pb pits induced by ion-probe analysis. For other samples the analyses were performed on the LA-ICPMS zircon mounts within the previously dated CL zone, in most cases directly adjacent to the ablation pits induced by U–Pb dating.

The system has been tuned (torch position, lenses, gas flows) on standard glass NIST 612 measuring ^{139}La, ^{232}Th and $^{232}Th^{16}O$ to get stable signals and high sensitivity on ^{139}La and ^{232}Th peaks, as well as low oxide rates ($^{232}Th^{16}O/^{232}Th \sim 0.1$ %) during ablation. The NIST 612 glass was used as an external standard (using the preferred values of the GeoReM reference material database, version 11/2006). Groups of five unknowns were bracketed with two calibration standards on both sides to track instrumental drift. The 91500 standard zircon (Wiedenbeck *et al.* 1995) was also measured in all sessions along with the unknowns to monitor accuracy. Results are summarized in the last columns of Table 3. Concentrations of measured elements were calculated using the Glitter software (e.g. Griffin *et al.* 2008). Precision is usually better than 10 % but depends on the absolute concentration. Elemental abundances were normalized to total Hf concentrations that were determined with a JEOL 8900M Superprobe adjacent to the ablation pits, using natural and synthetic calibration standards. Analytical conditions were 15 kV accelerating potential, a beam current of 15 nA, a spot size of ~ 1 μm, and a counting time of 10 s on peaks and 5 s on background.

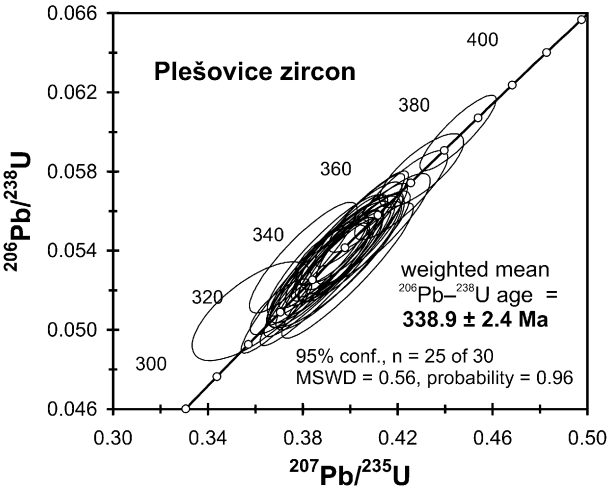

Figure 2. Concordia plot for results of the Plešovice zircon standard with weighted mean average.

SHRIMP and representative LA-ICPMS results are reported in Tables 1, 2 and 3. For additional LA-ICPMS data see online Appendix Tables A2 and A3, available at http://journals.cambridge.org/geo.

5. Results

5.a. CL characteristics

Zircon populations of eclogites (samples 5301 5302, 5306, NW-1 and 1111) consist of two different types. Type 1 zircon is very low luminescent or CL dark and shows diffuse internal features, gradually fading out textures, or faint growth zoning (Fig. 3a). Some grains are almost featureless. The type 1 zircon population includes brown, anhedral grains that often are broken into fragments, and subhedral, mostly turbid grains. Type 2 zircons form euhedral and clear single grains or overgrowths on type 1 zircon. Type 2 zircon is moderately luminescent, lacks remnants of igneous

https://doi.org/10.1017/S0016756809990665 Published online by Cambridge University Press

Table 3. LA-ICPMS trace element data for zircons from eclogites and granulites

Sample	5301	5301	5301	5301	5301	5301	5301	5301	5301	5301	5301	5301	5301	5301	5301	5301
Spot	3–1	8–1	5–1	6–1	7–1	13–1	1–1	10–1	11–1	4–1	14–1	12–1	9–1	20–1	2–1	21–1
CL type	1	1	1	1	1	1	1	2	2	2	2	2	2	2	2	2
Sc	984	1186	896	1002	996	892	938	1110	1202	1006	942	932	1000	1123	1029	1185
Ti	8.75	10.7	10.1	9.74	12.4	8.28	6.24	14.2	5.62	14.5	8.92	8.40	4.36	13.3	10.5	6.40
Y	2612	3465	2190	4329	3669	6235	4355	68.1	57.3	119	55.4	27.7	23.3	61.1	83.2	35.6
Nb	2.70	5.94	2.31	2.87	2.63	5.89	3.09	0.835	0.766	0.795	0.771	0.776	0.944	0.787	0.792	0.958
La	0.030	0.222	0.030	0.552	0.244	0.048	0.232	0.003	0.008	0.005	0.001	0.006	0.001	0.003	0.012	0.002
Ce	25.8	41.1	19.3	35.5	31.2	52.7	28.8	1.79	0.190	5.43	1.62	1.21	0.137	0.417	1.57	0.861
Pr	0.146	0.434	0.082	0.634	0.462	0.477	0.519	0.026	0.000	0.069	0.011	0.010	0.002	0.006	0.030	0.007
Nd	2.53	4.62	1.65	9.00	6.55	8.01	8.81	0.51	0.04	1.76	0.24	0.24	0.01	0.12	0.63	0.12
Sm	7.84	9.97	4.69	15.3	11.8	17.6	15.7	1.69	0.229	4.41	1.43	0.616	0.117	0.650	1.97	0.572
Eu	1.16	1.43	0.505	1.99	1.34	1.35	2.23	1.20	0.347	2.09	0.811	0.434	0.106	0.606	1.19	0.373
Gd	69.7	83.8	43.1	112.1	93.9	139	109	6.36	3.60	11.7	4.89	2.19	1.12	4.52	6.65	2.39
Tb	17.7	22.2	11.9	28.7	24.0	37.5	29.1	1.23	0.78	2.08	0.93	0.38	0.31	0.97	1.35	0.48
Dy	238	295	161	358	302	483	367	9.13	7.19	15.89	7.10	3.35	2.64	7.66	10.7	4.04
Ho	87.3	109	62.2	129	108	180	137	1.97	1.76	3.57	1.60	0.784	0.632	1.81	2.60	0.975
Er	417	496	305	581	474	839	624	6.63	5.76	11.0	5.04	2.61	2.19	5.65	8.49	2.98
Tm	88.6	111	68.1	118	99.1	184	129	1.08	1.07	1.84	0.869	0.453	0.365	1.06	1.35	0.560
Yb	784	954	613	976	824	1574	1119	8.56	9.05	12.4	6.50	3.19	2.93	8.18	11.1	4.18
Lu	127	158	104	164	131	261	186	1.21	1.38	1.79	1.00	0.562	0.606	1.20	1.79	0.603
Hf	10345	10345	9837	10769	7717	8056	9243	10939	13313	10345	11702	9752	12465	9921	10939	13144
Ta	1.24	2.11	1.41	1.15	0.800	2.58	1.16	0.120	0.116	0.077	0.124	0.103	0.118	0.104	0.112	0.091
Pb	105	152	103	192	193	428	198	39.6	11.3	93.1	69.0	28.7	18.7	26.0	47.0	18.5
Th	233	427	203	511	610	1269	441	3.33	0.346	11.4	3.65	1.87	0.376	0.939	3.32	1.31
U	296	422	291	522	510	972	464	173	42.7	297	286	105	70.5	33.2	147	49.8
Th/U	0.79	1.01	0.70	0.98	1.20	1.31	0.95	0.02	0.01	0.04	0.01	0.02	0.01	0.03	0.02	0.03
REE total	1865	2287	1396	2530	2108	3778	2757	41.4	31.4	74.1	32.0	16.0	11.2	32.8	49.5	18.1
Yb_N/Sm_N	93.2	89.3	121.9	59.6	65.2	83.6	66.7	4.73	36.9	2.63	4.24	4.83	23.4	11.7	5.26	6.82
Eu/Eu^*	0.151	0.151	0.109	0.147	0.123	0.083	0.165	1.12	1.17	0.890	0.938	1.14	0.895	1.08	1.01	0.975
Ce/Ce^*	93.1	31.9	93.8	14.4	22.3	83.9	20.0	53.5		72.4	138	38.5	28.7	22.2	19.6	52.4
Sm_N/La_N	410	71.4	249	44.0	76.8	582	107	1075	48.5	1492	3031	175	211	323	253	395
Lu_N/Gd_N	14.6	15.2	19.5	11.8	11.2	15.1	13.7	1.53	3.08	1.23	1.64	2.06	4.35	2.13	2.17	2.03
Ti-in-zircon, °C	783	804	797	794	819	777	750	780	694	782	735	730	673	773	751	706
U/Pb age (Ma)	459	421	462	464	443	473	481	345	355	345	n.a	344	347	507	339	402

Table 3. (*Cont.*)

Sample	5312	5312	5312	5312	5312	5312	5312	5312	5312	5312	5312	5312	5312	5312	5312	5312
Spot	2–1	1–1	3–1	4–1	5–1	12–1	11–1	10–1	7–1	6–1	8–1	9–1	77	80	46	58
CL type	1	1	1	1	1	1	1	1	1	1	1	1	1	1	1	1
Sc	972	1285	929	911	1021	997	997	1043	1104	1004	1139	1052	768	887	701	778
Ti	16.1	21.6	26.7	20.6	18.3	25.9	25.2	18.5	11.3	8.43	24.8	21.6	23.1	32.1	12.6	135.6
Y	1883	2733	1076	2237	1768	3039	1550	1718	1349	1441	1714	1724	1457	1689	947	1540
Nb	2.85	5.53	3.24	5.06	2.33	8.37	2.79	4.36	3.33	2.03	4.24	3.82	2.58	2.06	1.89	3.75
La	0.037	15.8	6.92	2.48	27.5	0.639	9.03	0.246	1.30	0.055	0.111	6.41	26.2	43.4	5.2	0.253
Ce	10.1	58.2	28.9	16.5	51.8	34.9	22.0	11.6	12.5	7.9	11.6	25.0	53.0	75.4	14.8	16.4
Pr	0.136	5.360	2.050	0.300	4.330	0.509	1.423	0.124	0.336	0.087	0.101	1.598	4.560	8.440	1.010	0.199
Nd	2.83	24.53	8.84	2.92	17.58	4.87	5.78	1.49	2.07	1.56	1.52	10.33	17.00	32.06	4.37	2.05
Sm	6.42	11.1	3.07	5.81	7.68	9.83	4.77	4.04	2.84	4.44	4.00	5.79	5.14	6.87	2.01	3.28
Eu	0.508	1.00	0.392	0.724	0.730	0.883	0.500	0.358	0.294	0.447	0.537	0.590	0.474	0.745	0.182	0.257
Gd	45.7	63.8	22.4	55.8	45.8	76.8	33.0	33.6	27.4	37.6	34.6	39.0	31.4	38.0	19.2	33.3
Tb	12.0	16.9	5.99	15.2	11.9	20.5	8.70	9.08	7.15	9.55	9.18	10.4	7.70	9.30	4.93	8.73
Dy	150	217	81.9	197	147	253	112	126	99.6	120	125	136	108	129	73.4	122
Ho	55.1	81.5	32.3	73.7	55.2	90.5	42.1	48.8	37.6	45.0	50.0	51.8	43.4	51.1	29.9	48.1
Er	256	388	162	348	262	421	206	245	188	209	240	253	217	251	157	233
Tm	57.3	86.0	38.1	75.1	59.7	89.2	50.0	55.8	44.6	47.6	58.5	59.4	50.7	57.1	37.6	52.1
Yb	517	798	388	684	573	799	477	546	462	469	588	595	480	544	379	480
Lu	85.5	134.2	68.1	110	93.8	126	86.7	97.0	81.0	80.8	103	100	90.1	106	76.9	89.5
Hf	9073	11872	10176	9413	10345	9073	9921	10430	11278	12041	9497	10600	10261	12211	10261	12211
Ta	0.879	1.72	1.21	1.69	0.904	2.71	0.867	1.29	1.47	0.901	1.32	1.41	1.21	0.907	1.12	1.69
Pb	129	220	82.5	198	166	313	158	136	211	98.8	133	125	122	140	111	151
Th	139	297	100	213	169	530	140	117	153	88.1	93.8	138	131	163	95.6	226
U	387	560	296	657	489	932	558	475	499	259	385	451	403	486	340	535
Th/U	0.36	0.53	0.34	0.32	0.34	0.57	0.25	0.25	0.31	0.34	0.24	0.31	0.33	0.34	0.28	0.42
REE total	1198	1902	849	1586	1357	1928	1060	1179	967	1034	1226	1295	1135	1353	805	1089
Yb_N/Sm_N	75.1	67.3	118	110	69.7	75.8	93.2	126	152	98.6	137	95.9	434	324	965	795
Eu/Eu^*	0.091	0.115	0.145	0.123	0.119	0.098	0.122	0.094	0.102	0.106	0.140	0.120	3.74	3.29	4.61	5.07
Ce/Ce^*	34.1	1.52	1.85	4.59	1.14	14.7	1.48	16.0	4.55	27.7	26.4	1.88	0.867	0.980	0.718	0.196
Sm_N/La_N	273	1.11	0.705	3.72	0.444	24.5	0.840	26.1	3.48	129	57.3	1.44	0.3	0.252	0.616	20.6
Lu_N/Gd_N	15.1	16.9	24.4	15.8	16.5	13.2	20.8	23.3	23.8	17.3	24.0	20.7	23.1	22.4	32.3	21.6
Ti-in-zircon, °C	848	882	909	877	862	904	901	864	809	779	899	883	890	932	820	1157
U/Pb age (Ma)	412	452	337	357	400	400	367	395	480	492	392	407	413	418	474	479

Table 3. (*Cont.*)

Sample	5312	5312	5312	5312	5312	5312	5312	5312	5312	5312	5312	91500 GEOREM 01/2008		91500 This study, n=13	
Spot	25	22	1–2	20–1	21–1	5–2	23–1	24	26	20	35				
CL type	1	1	2	3	2	2	2	3	3	3	3	Mean	SD	Mean	SD
Sc	857	834	1001	1090	1071	1137	1033	896	858	885	885				
Ti	16.3	13.0	29.7	25.5	28.8	35.0	34.6	45.2	43.7	44.7	50.2	6	1	6.1	0.5
Y	1289	2203	80.1	24.8	56.3	109.1	40.7	109	106	113	176				
Nb	1.54	1.61	1.15	1.12	1.75	1.11	0.935	2.43	3.44	2.26	3.02				
La	2.08	0.422	0.148	0.026	0.041	0.286	0.032	0.019	0.297	0.015	0.062	0.006	0.003	0.005	0.004
Ce	9.8	11.3	47.8	36.0	25.6	43.8	32.3	2.8	5.6	2.3	2.6	2.6	0.3	2.7	0.6
Pr	0.469	0.185	0.449	0.208	0.166	0.385	0.335	0.026	0.216	0.031	0.076	0.024	0.015	0.013	0.005
Nd	3.30	2.69	6.88	2.82	2.03	4.85	4.37	0.62	1.63	0.61	1.13	0.24	0.04	0.22	0.04
Sm	3.23	6.01	7.77	3.47	1.88	4.29	5.30	1.83	2.32	1.95	2.74	0.5	0.08	0.46	0.10
Eu	0.357	0.512	1.13	0.540	0.500	1.01	0.900	0.814	0.706	0.723	1.01	0.24	0.03	0.23	0.07
Gd	29.2	53.0	10.8	4.23	4.11	8.70	7.22	8.30	7.23	7.92	12.1	2.2	0.3	3.5	0.4
Tb	7.56	13.9	1.72	0.629	0.820	1.60	1.02	1.62	1.54	1.52	2.59	0.86	0.07	0.88	0.11
Dy	104	181	10.9	3.48	6.78	13.0	5.50	13.9	12.2	12.8	22.1	12	1	12.5	1.1
Ho	40.3	67.9	2.23	0.628	1.69	3.06	1.03	3.19	3.01	3.17	5.18	4.8	0.4	4.96	0.44
Er	192	321	7.38	2.04	5.74	10.3	2.94	11.2	10.9	11.1	19.1	25	3	26.6	2.3
Tm	45.7	71.7	1.25	0.310	1.10	1.74	0.566	2.09	2.09	2.18	3.29	6.9	0.4	7.18	0.51
Yb	446	667	9.88	2.56	9.01	12.4	4.22	17.6	16.5	18.0	28.2	74	4	76	6
Lu	73.4	109	1.33	0.314	1.23	1.66	0.555	2.45	2.51	3.00	4.06	13	1	13	1
Hf	10261	10685	13992	13398	12041	13144	14076	12635	12635	12889	12296				
Ta	0.825	0.796	0.159	0.149	0.560	0.164	0.175	1.22	3.56	1.68	2.76				
Pb	94.2	118	61.0	30.6	28.8	55.3	47.0	207	262	204	243				
Th	93.7	163	245	93.7	135	326	137	8.80	35.3	15.3	19.7				
U	306	367	134	114	104	181	171	802	1040	800	949				
Th/U	0.31	0.44	1.83	0.82	1.29	1.81	0.80	0.01	0.03	0.02	0.02				
REE total	957	1507	110	57.2	60.7	107	66.3	66.4	66.6	65.5	104				
Yb_N/Sm_N	469	487	1.19	0.688	4.47	2.69	0.743	6.87	8.12	9.47	9.21				
Eu/Eu^*	4.05	4.53	0.377	0.431	0.550	0.507	0.445	1.65	1.58	1.72	1.71				
Ce/Ce^*	0.470	0.191	44.6	118	74.5	31.75	75.5	0.112	0.410	0.146	0.253				
Sm_N/La_N	2.47	22.6	83.5	215	72.4	23.8	267	153	12.4	211	70.3				
Lu_N/Gd_N	20.2	16.6	0.989	0.597	2.41	1.53	0.618	2.37	2.79	3.05	2.70				
Ti-in-zircon, °C	849	824	859	842	856	879	877	910	906	909	924				
U/Pb age (Ma)	468	478	341	335	382	330	353	339	344	335	345				

Concentrations in ppm. $Eu/Eu^* = Eu_N/\sqrt{(Sm_N{}^*Gd_N)}$, $Ce/Ce^* = Ce_N/\sqrt{(La_N{}^*Pr_N)}$, normalization to chondrite after Boynton (1984).
Ti-in-zircon temperatures after Ferry & Watson (2007), assuming $a_{SiO2} = 1$ and $a_{TiO2} = 0.6$ for magmatic zircon (CL type 1 and 4) and $a_{SiO2} = 1$ and $a_{TiO2} = 1$ for metamorphic zircon (CL type 2 and 3).

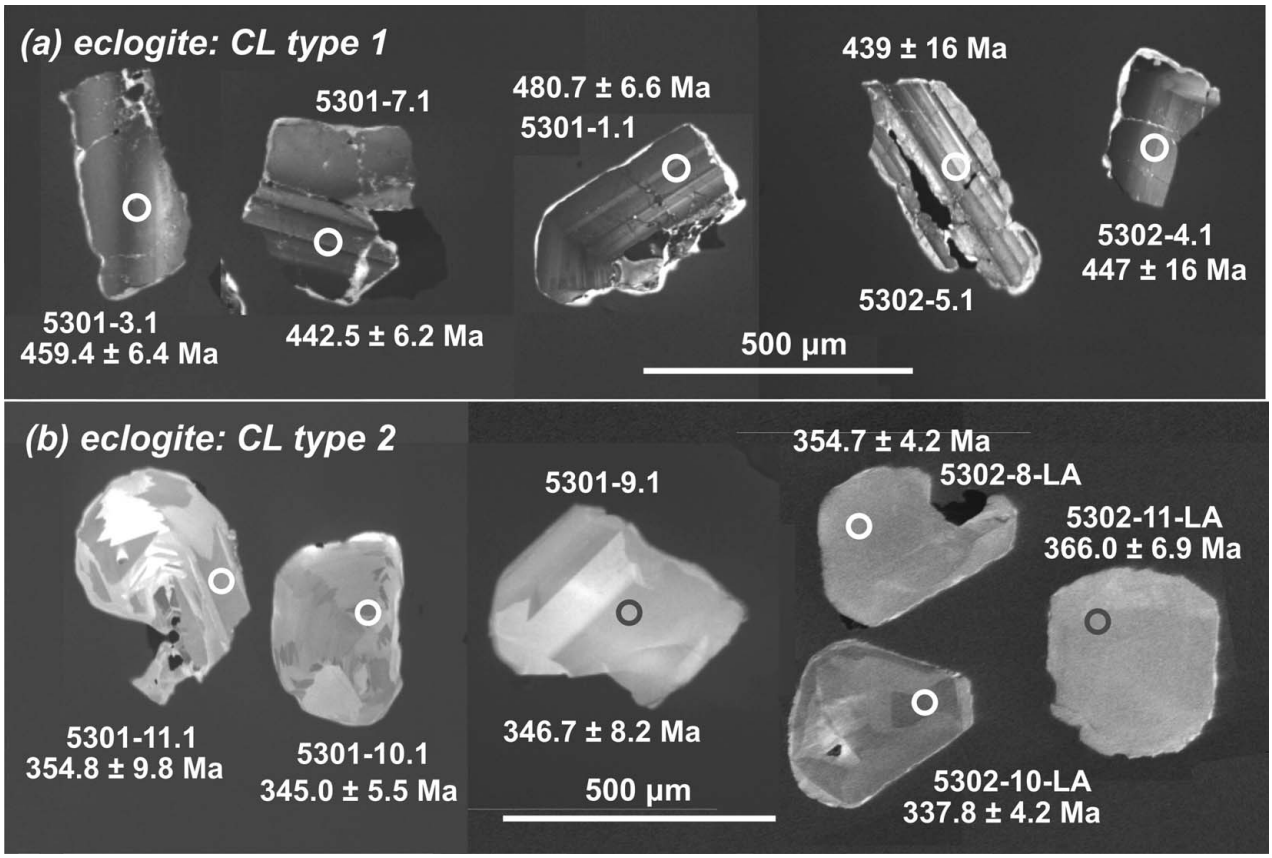

Figure 3. Cathodoluminescence images of representative zircons from eclogites with SHRIMP and LA-ICPMS ages and spot identification number. Ages are reported with 1σ uncertainty.

zoning and displays a variety of CL structures that comprise diffuse and blurred zoning patterns, patchy, sector and fir-tree zoning (Fig. 3b).

Zircons of the granulite sample 5312 show three different types of CL patterns. Type 1 zircons are moderately luminescent, oscillatory zoned grains that often are replaced and rimmed by zircon of type 2 and type 3 (Fig. 4a). Many grains are fractured and strongly corroded. Type 2 zircon is characterized by homogeneous, diffuse or broad patchy zoning patterns, and occurs as single grains or overgrowth around type 1 and type 3 zircon. Type 3 zircons (Fig. 4b) are represented by non-fractured, low luminescent, dark grains that show broad homogeneous domains, patchy CL features or faint growth zoning of variable width.

The zircon populations of granulite sample 1106 consist of anhedral to subhedral grains with variable shapes from rounded to more elongated types. Many grains are fractured. CL imaging revealed internal structures with broad homogeneous domains and sector-zoning (Fig. 4c). Many grains are surrounded by thin overgrowths, which are too small to analyse. Distinct cores were not recognized. Internal features generally have a faint and washed-out appearance. This population is described as type 4 zircon.

5.b. SHRIMP and LA-ICPMS U–Pb geochronology

In order to constrain protolith and metamorphic ages, ion-microprobe U–Pb analyses of three samples (38 spot analyses) and LA-ICPMS dating of six samples (366 spot analyses) were carried out. Results for two representative samples are summarized in Tables 1 and 2 and depicted in Figures 5 and 6. Additional LA-ICPMS data are compiled as Table A2 in the online Appendix at http://journals.cambridge.org/geo.

The new data document a large age variability within all studied samples. In eclogites from Międzygórze (5301, 5302), apparent ^{206}Pb–^{238}U ages range from 329 to 599 Ma (n = 66) and from 320 to 408 Ma (n = 21), respectively (Figs 5a, b, 6). The relatively small dataset of sample 5302 is biased because grain selection was focused on presumably metamorphic zircon. In eclogites from Nowa Wieś (1111, NW-1), ^{206}Pb–^{238}U ages vary between 377 and 533 Ma (n = 43) and between 310 and 609 Ma (n = 69), respectively (Fig. 6c, d). The granulites from the Stary Gierałtów area show a similar distribution of apparent ages (sample 1106: 335–531 Ma, n = 79; sample 5312: 292–538 Ma, n = 88) (Fig. 6e, f).

In all samples, most spots are less than 10 % discordant, and there is no obvious correlation between

https://doi.org/10.1017/S0016756809990665 Published online by Cambridge University Press

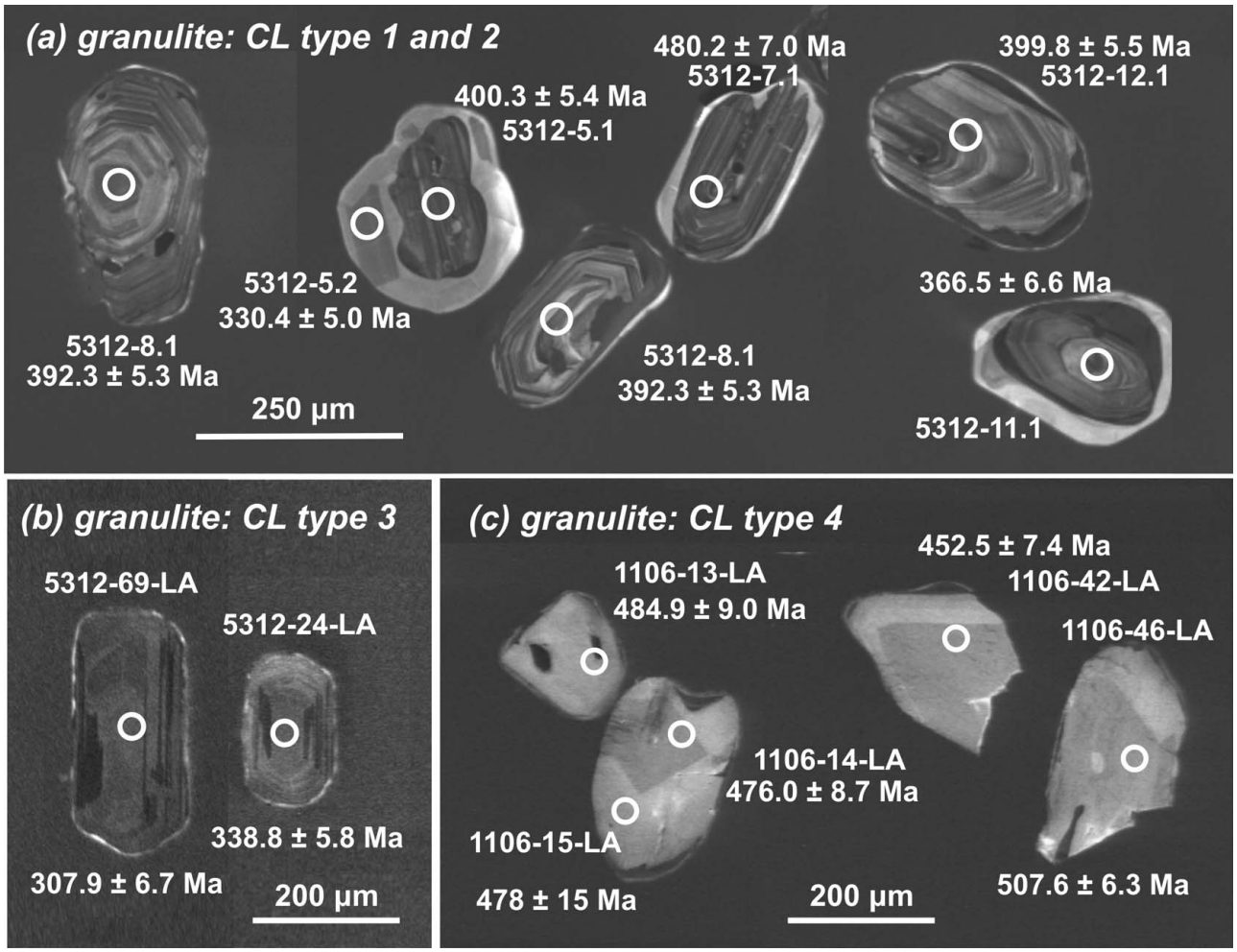

Figure 4. Cathodoluminescence images of representative zircons from granulites with SHRIMP and LA-ICPMS ages and spot identification number. Ages are reported with 1σ uncertainty.

apparent age and U concentration. Data points are distributed along concordia between *c.* 290 and *c.* 610 Ma without extreme outliers. Probability density distribution diagrams show several peaks (Fig. 7). Neither at the upper nor the lower end of the age spectra do homogeneous age groups occur which would allow a straightforward interpretation as protolith and/or metamorphic ages. Most data points for type 1 and type 4 zircon grains scatter along concordia between *c.* 400 and 600 Ma. In contrast, type 2 and 3 zircon grains mostly indicate younger apparent U–Pb ages that cluster at *c.* 330–340 Ma and *c.* 370 Ma. In general, there seems to be a younging trend from Cambro-Ordovician ages towards 330–340 Ma, which represents the well-established age of Variscan metamorphism in the study area. Maximum apparent ages in three samples (1111, 5312, 1106) are *c.* 530–535 Ma. For the eclogite samples 5301 and NW-1, the oldest grains indicate an age of *c.* 600–610 Ma.

5.c. Trace element characteristics

Based on chondrite-normalized REE distribution patterns, the zircon populations can be subdivided into two well-defined groups which closely correlate to distinct CL features. Type 1 and type 4 zircon grains of both rock types are characterized by positive Ce and negative Eu anomalies, and steep HREE slopes ($Lu_N/Gd_N = 8.1–32.3$) (Fig. 8a–d, f, g; Tables 3, A3). In two samples (5312, 1111), some type 1 grains show flat LREE patterns with a negative slope (Fig. 8d, h), possibly indicating accidental analysis of apatite micro-inclusions. Compared to grains with other CL features, concentrations of total REEs (eclogites: 555–6945 ppm; granulites: 413–1928 ppm), Y (eclogites: 910–11425 ppm; granulites: 524–3039 ppm) and Th (eclogites: 127–6496 ppm; granulites: 28–530) are high (Tables 3, A3). U contents vary between 135–2896 ppm (eclogites) and 74–932 ppm (granulites). Th/U ratios range from 0.56–2.24 (eclogites) and from 0.24–0.68 (granulites).

Type 2 and type 3 zircon grains are characterized by flat HREE patterns ($Lu_N/Gd_N = 0.6–4.4$) and a positive Ce anomaly (Fig. 8a–c, e, g; Table 3, A3). Eu anomalies are practically absent ($Eu/Eu^* = 0.4–1.7$). Zircon grains of these groups have low concentrations of total REE (eclogites: 11–157 ppm; granulite: 57–110 ppm), Y (eclogites: 17–197 ppm; granulite: 25–176 ppm) and Th (eclogites: < 1–39 ppm; granulite: 9–326 ppm). U contents vary between 33–3131 ppm

https://doi.org/10.1017/S0016756809990665 Published online by Cambridge University Press

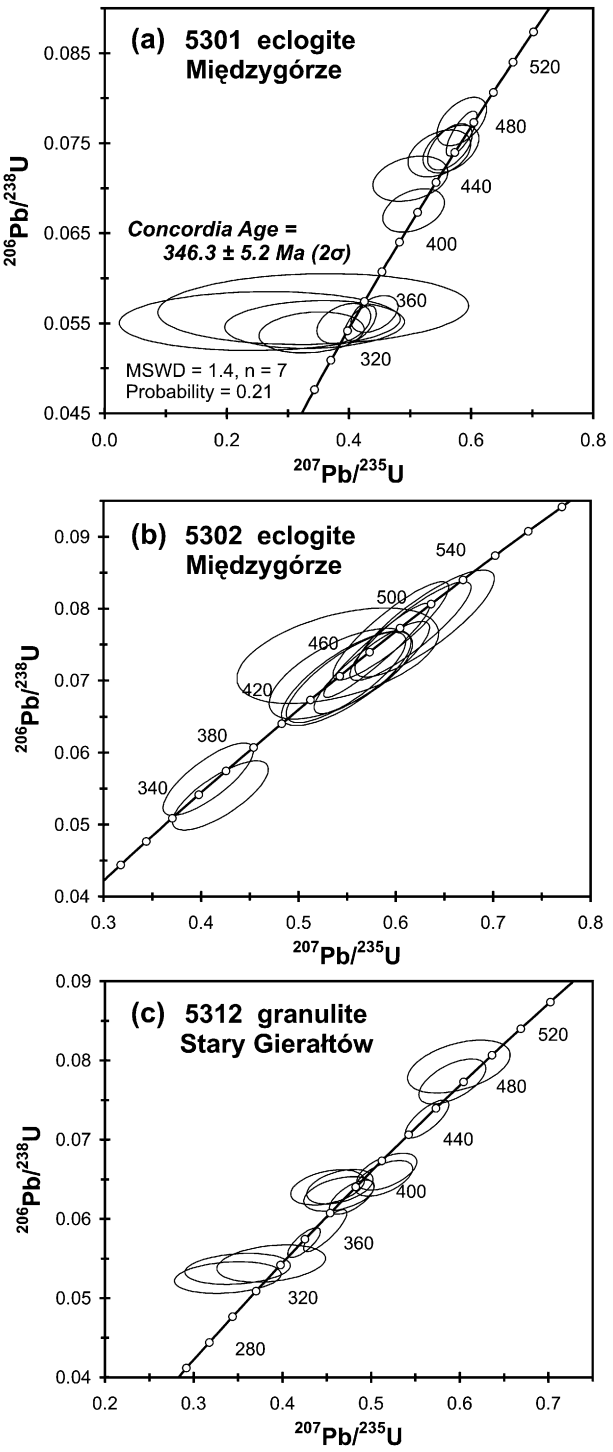

Figure 5. U–Pb concordia diagrams showing SHRIMP analytical data of samples 5301, 5302 and 5312. Data point error ellipses indicate 2σ uncertainties.

(eclogites) and 74–932 ppm (granulite). In eclogites, Th/U ratios generally are very low (< 0.01–0.18), whereas Th/U ratios of the granulite sample 5312 are more variable (< 0.01–1.83) (Table 3).

For type 1 and 4 zircon grains of both rock types, Ti-in-zircon thermometry (Ferry & Watson, 2007) yielded apparent temperatures of about 790 to 870 °C. Ti-in-zircon temperatures for type 2 and type 3 zircon of eclogites, uncorrected for pressure, fall within the range of 690–820 °C; such zircons from granulite sample 5312 indicate a temperature of about 885 °C.

6. Discussion

6.a. Magmatic v. metamorphic zircon origin

CL imaging revealed four types of zircon: (1) oscillatory-zoned or relatively homogeneous grains with very low to moderate luminescence and without visible inherited cores, (2) moderately luminescent overgrowths and single grains showing a range in internal structures, including relatively homogeneous CL domains, faint and blurred zoning patterns, sector and fir-tree zoning, (3) low luminescent or dark grains that show broad homogeneous domains, patchy CL features or faint growth zoning of variable width, and (4) grains with broad homogeneous CL domains and sector-zoning with a general faint and washed-out appearance. Type 1 and 4 zircon grains are interpreted to be of magmatic origin, whereas type 2 and 3 zircon grains are related to metamorphic processes. In the case of all eclogites, presumed metamorphic and magmatic origins correspond well to extremely low Th/U ratios for overgrowths and related single grains, and moderate Th/U values for protolith zircon. This is not entirely correct for metamorphic zircon of granulite 5312, which has highly variable Th/U ratios up to 1.83 (Table 3). However, the Th/U ratio in zircon is often strongly influenced by protolith characteristics and/or the local chemical environment of formation (e.g. Harley, Kelly & Möller, 2007 and references therein), and thus, not too much emphasis should be placed on this parameter to distinguish between magmatic and metamorphic modes of formation.

6.b. What is the reason for the scatter of data points along concordia?

The ^{206}Pb–^{238}U dates for zircon grains of all studied samples show a large variability, and no single age can be calculated. Protolith ages and the time of metamorphic overprints cannot directly be deduced from the new data. Although spot selection was guided by CL images, it cannot be ruled out that some of the scatter is an artifact of beam overlap on neighbouring growth zones producing mixed ages. However, both the LA-ICPMS and SHRIMP datasets show a similar age variability, despite the fact that these techniques exploit considerably different sample volumes. Judging from the CL images, it is considered unlikely that mixing is the major cause for the diffuse distribution of data points. Instead, it is suggested that Pb-loss mainly controls this spread along concordia. A large spread in apparent ages along concordia has already been described in a previous SHRIMP study by Lange *et al.* (2005*a*) for the granulite 1106 from Stary Gierałtów. These authors observed no correspondence between degree of apparent resetting and U concentration, and they therefore concluded that non-metamict

https://doi.org/10.1017/S0016756809990665 Published online by Cambridge University Press

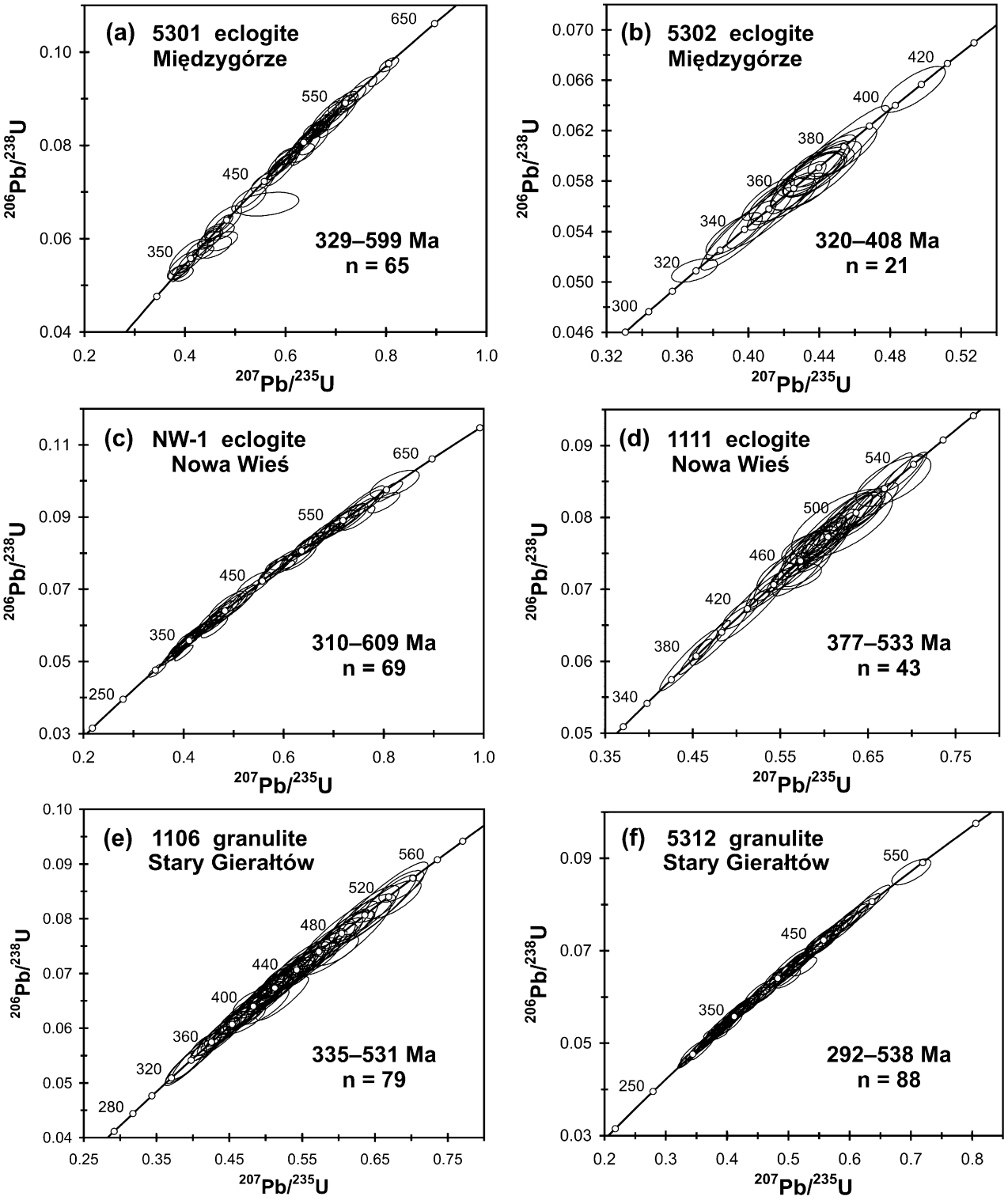

Figure 6. U–Pb concordia diagrams showing LA-ICPMS zircon data of eclogites and granulites. Data point error ellipses indicate 2σ uncertainties.

magmatic protolith zircon experienced variable Pb-loss during Variscan high-grade metamorphism at *c.* 340 Ma and/or *c.* 360 Ma. The postulated relationship between resetting and Variscan metamorphism is a plausible interpretation, due to the presence of a distinct younging trends towards an age that is typically associated with the Variscan metamorphic overprint. However, the resetting of presumably non-metamict zircon demands further explanation. Due to the high closure temperature for diffusion of Pb in zircon (> 900 °C; Lee, Williams & Ellis, 1997; Cherniak & Watson, 2001), there are not many possibilities to reset non-metamict zircon under normal crustal conditions. Ashwal, Tucker & Zinner (1999) argued that volume and/or fracture-assisted diffusional resetting is possible, if the blocking temperature for

https://doi.org/10.1017/S0016756809990665 Published online by Cambridge University Press

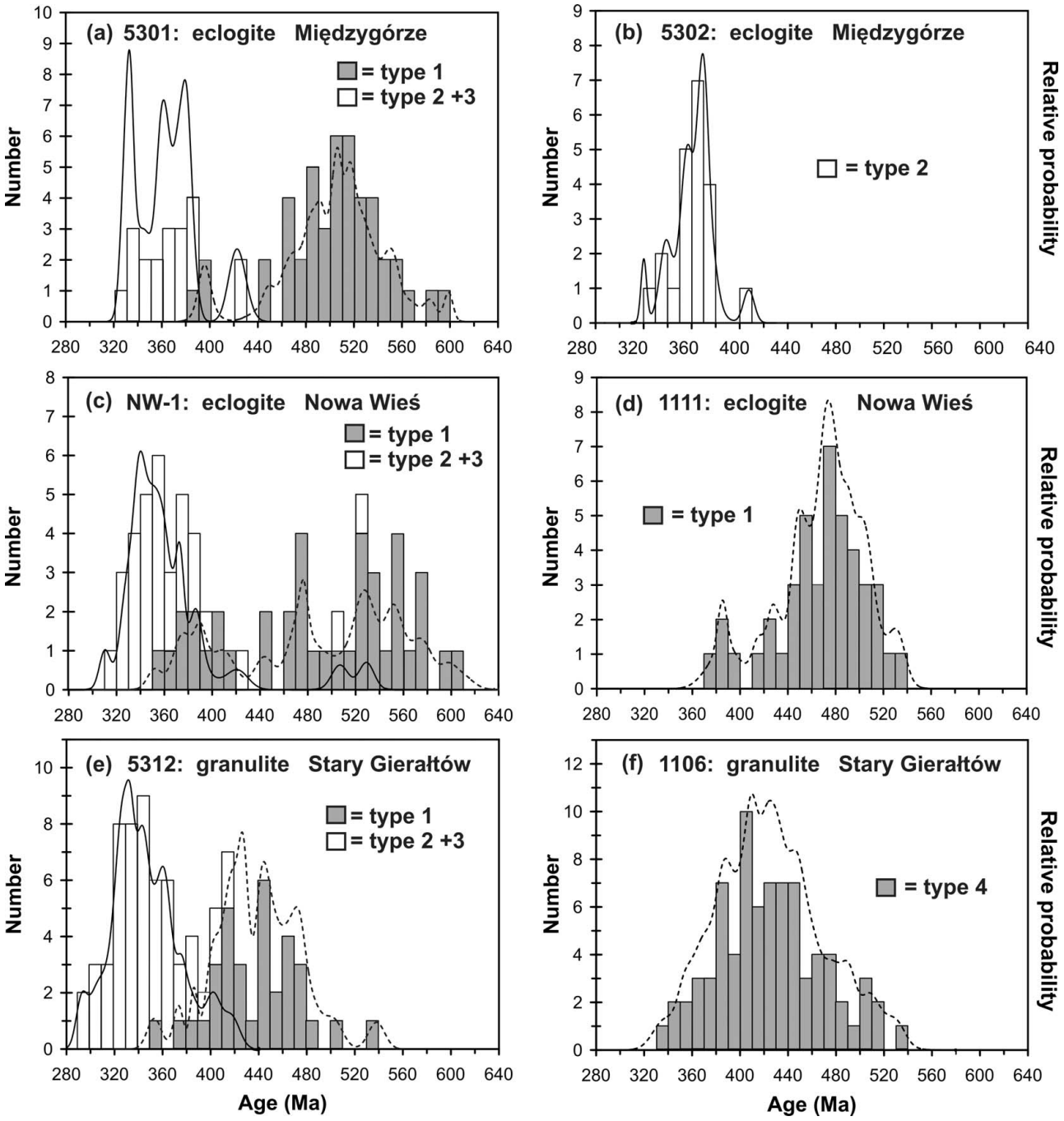

Figure 7. Normalized probability distribution diagrams with stacked histograms for LA-ICPMS zircon data of eclogites and granulites. Bin width = 10 Ma.

zircon is exceeded for a long time span, or if zircon has been repeatedly affected by granulite- to amphibolite-facies metamorphism. Lange *et al.* (2005*a*) considered protracted or multiple high-grade metamorphism as a realistic scenario for the Orlica-Śnieżnik complex, but noted that unambiguous geochronological evidence for such a background had not been established at the time of their study. This situation has changed. Previous Sm–Nd and U–Pb geochronology of granulites yielded ages of *c.* 350–330 Ma (Brueckner, Medaris & Bakun-Czubarow, 1991; Klemd & Bröcker, 1999; Štípská, Schulmann & Kröner, 2004; Lange *et al.* 2005*a*), and this age group has mostly been related to short-duration (U)HP metamorphism. However, a recent Lu–Hf and Sm–Nd chronometric study of granulites from the Stary Gierałtów area presented convincing arguments that (U)HP conditions were already attained at some point between *c.* 387–360 Ma (Anczkiewicz *et al.* 2007). These authors related the *c.* 340 Ma ages to a high temperature metamorphic episode under lower pressures on the retrograde *P–T* path. Although the geological significance of the 340 Ma ages (eclogite stage or subsequent overprinting) remains controversial (Bröcker *et al.* 2009), it is obvious from the Lu–Hf data that the time span during which the granulites experienced high-grade metamorphic conditions is

https://doi.org/10.1017/S0016756809990665 Published online by Cambridge University Press

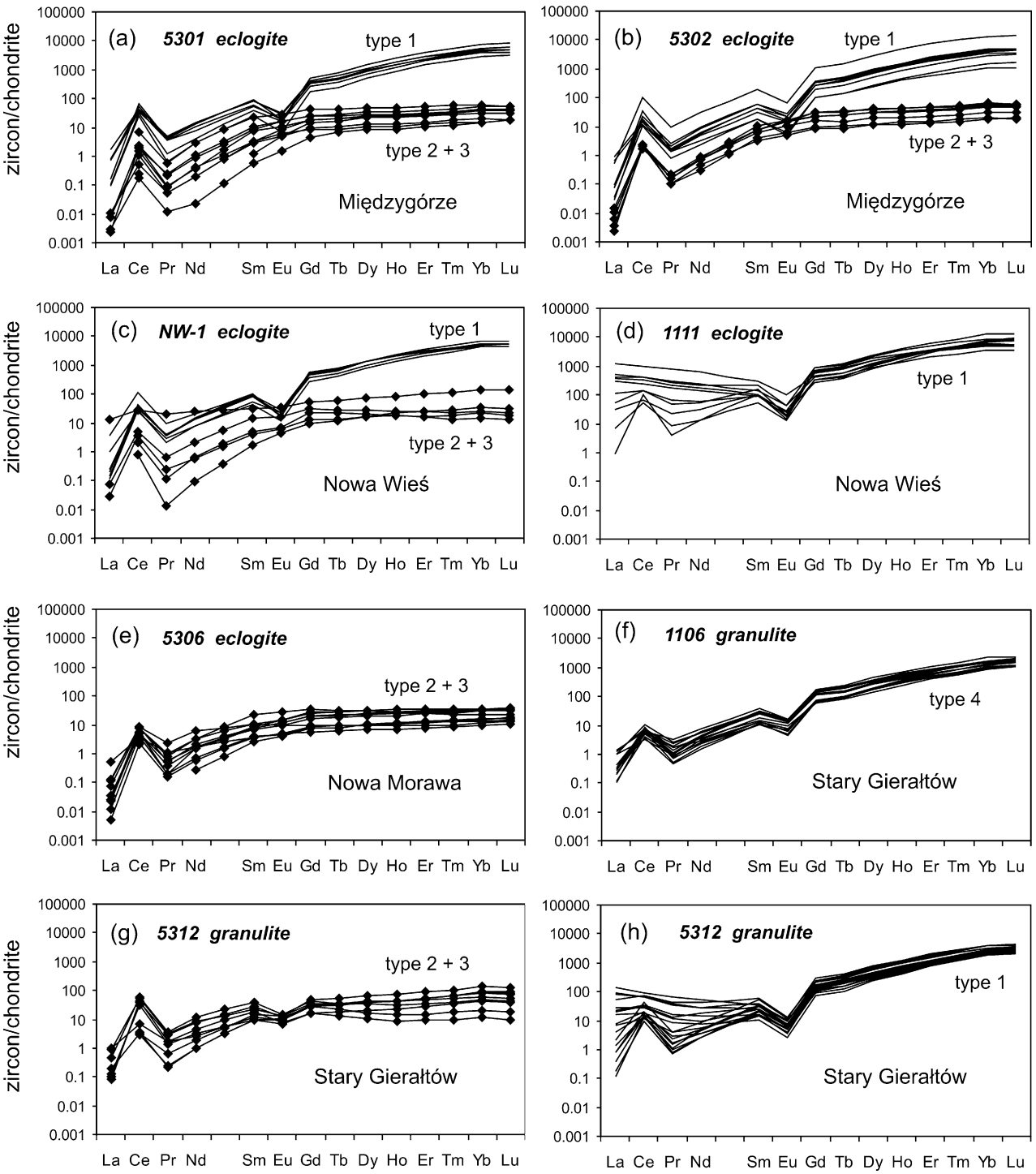

Figure 8. Chondrite-normalized REE patterns of eclogites and granulites from the Orlica-Śnieżnik complex. Normalization to chondrite after Boynton (1984). Line represents magmatic zircons (type 1 or 4); line with diamond symbols represents metamorphic zircon (type 2 and 3). For better visualization, results for sample 5312 are shown in two different diagrams (g, h).

much longer than previously assumed. Thus, the geological context for the granulites seems to agree with conditions that have been shown elsewhere to permit Pb-loss in non-metamict zircon. There are indications that the eclogites have also been affected by prolonged and/or multiple HT events, but for this rock type a different interpretation is more plausible. In the eclogites, many type 1 zircon grains have a very low luminescence, and grains with brown colour are common. These observations are consistent with a high degree of radiation damage, and suggest that in these rocks Pb-loss is mainly a consequence of partial metamictization. It is interesting to note that chondrite-normalized REE patterns of magmatic type 1 and type 4 zircon grains seem to be completely unaffected by the processes that have led to disturbance of the U–Pb system. Despite variable degrees of Pb-loss and partial age resetting, such zircons preserved an igneous

https://doi.org/10.1017/S0016756809990665 Published online by Cambridge University Press

REE signature, whereas all metamorphic zircons (type 2 and 3; mostly 330–380 Ma) show flat HREE patterns (Fig. 8). There are no transitional types between both groups.

6.c. What is the protolith age of eclogites and granulites?

We expected that for each sample, a relatively small number of ion-probe analyses (~ 10–15) would be sufficient to determine homogeneous age groups for the central grain parts of igneous zircon. However, due to the considerable spread in apparent U–Pb ages, no single age group could be defined for the first three samples studied, indicating the need for a different analytical strategy. The oldest date for each sample may be used as approximation to the protolith age, but it is not really convincing to place geological significance on a single spot analysis that may be compromised by inheritance or Pb-loss. A cluster of dates would allow a more robust interpretation (e.g. Gehrels, Valencia & Pullen, 2006). In order to achieve this objective, a large number of spots were analysed by LA-ICPMS.

Although a comprehensive U–Pb dataset is now available, the protolith ages still remain obscure due to the lack of a well-defined age cluster at the upper end of the age spectra. Normalized probability diagrams and histograms (Fig. 7) document the complexity of this dataset for individual samples by indicating apparent peaks with unclear geological significance between the well-established age of Variscan metamorphism (*c.* 330–340 Ma) and the upper end of the age spectra, which most likely includes the time of protolith formation. Such complex age patterns are typical for detrital zircon populations, however, at least for the eclogites and the mafic granulite (1106) a sedimentary origin is unrealistic. These rocks are considered to be derivatives of igneous mafic rocks, but the specific original rock type is unknown. For sample 5312 a tuffaceous origin cannot completely be ruled out. Judging from the similarity to the age patterns of samples derived from magmatic precursors and the lack of typical characteristics of sedimentary grains, the zircon population of sample 5312 is not considered to be significantly contaminated by detrital components.

It can be argued that U–Pb ID-TIMS dating, combined with a micro-drill and/or a chemical abrasion technique, has the potential to provide a higher precision of individual data points. However, this analytical approach would not significantly change the general picture. The main problem is not the analytical precision of the SHRIMP and LA-ICPMS dating methods, but variable and possibly multi-stage Pb-loss. Further complexities are added by metamorphic zircon growth and re-equilibration processes, and, to a minor extent, possible mixing of different aged domains during analysis. An additional problem is added by the possibility that inheritance may contribute to the spread in ages. Zircon populations of igneous mafic rocks commonly record no or only minimal inheritance, but examples documenting the presence of inherited components were repeatedly described (e.g. Pilot *et al.* 1998; Root *et al.* 2004; Peytcheva *et al.* 2008; Koglin, Kostopoulos & Reischmann, 2008; Presnyakov *et al.* 2008). All of these factors create a situation where accurate protolith ages cannot be determined with any precision. No solution to the problem is free from ambiguity.

At this point we attempt to outline two possible scenarios that assume no or only minor contamination by inherited components. We consider such circumstances to be very likely, but emphasize that in case of significant contamination by inherited components, other scenarios are possible. If the zircon populations are free of inheritance, the oldest age in each sample can be interpreted as the closest approximation to the true protolith age. This approach would indicate apparent magmatic crystallization ages of *c.* 531 and *c.* 538 Ma for the granulites, and of *c.* 533 Ma for eclogite sample 1111. The oldest grains of eclogites 5301 and NW-1 yield ages of *c.* 599 and *c.* 609 Ma, respectively. Accordingly, all samples would provide apparent protolith ages that are older than the precursors of the orthogneisses (*c.* 490–510 Ma; Oliver, Corfu & Krogh, 1993; Kröner *et al.* 2001; Turniak, Mazur & Wysoczanski, 2000; Štípská, Schulmann & Kröner, 2004), supporting interpretations that suggest tectonic juxtaposition of (U)HP rocks and their country rocks (e.g. Don *et al.* 1990; Don, 2001; Štípská, Schulmann & Kröner, 2004). In each sample, the one to two oldest ages represent single data points that are separated from the remaining population. Assuming that these ages are related to inheritance, it is possible to calculate homogeneous age groups based on the four to six oldest grains of the remaining population. For the eclogite samples 5301 and NW-1, this approach indicates protolith ages > 550 Ma (Fig. A1 of online Appendix; http://www.cambridge.org/journals/geo), whereas eclogite sample 1111 yields an apparent protolith age of 506 ± 6 Ma (Fig. A1). Granulite samples 1106 and 5312 provide apparent ages of 509 ± 9 Ma and 477 ± 7 Ma, respectively (Fig. A1). This would imply that the magmatic precursors of some (U)HP rocks formed largely coevally to the protoliths of the enclosing orthogneisses.

For now, all attempts to unravel protolith ages from this dataset lack definiteness. The time of igneous crystallization of the parent rocks cannot be resolved with confidence. Due to the general scarcity of eclogites and granulites in the Orlica-Śnieżnik complex and the good coverage of the main outcrops by our sample selection, we consider the prospects for determining accurate and precise protolith ages in future studies to be extremely small.

6.d. U–Pb ages and trace element characteristics of metamorphic zircon

The metamorphic evolution of the Sudetes, and in particular the Orlica-Śnieżnik complex, has been a matter of considerable debate. Several studies suggested

https://doi.org/10.1017/S0016756809990665 Published online by Cambridge University Press

a polymetamorphic history with discrete HT events that affected Cambrian protoliths during pre-Variscan and Variscan time, in addition to the well-established Carboniferous event (for the most recent overviews, see Żelaźniewicz *et al.* 2006; Bröcker *et al.* 2009, and references therein). The cumulative probability diagrams of all studied samples show several peaks between the presumed time of protolith formation and the 340 Ma event. Although it cannot be ruled out that these age patterns reflect to some extent distinct tectonometamorphic processes, it is impossible to verify such speculations. At this stage the most reasonable interpretation is to consider most of these peaks as geologically meaningless. The only exception is the accumulation of data points at *c.* 390–360 Ma (Fig. 7a–f; Fig. A1b), because such dates were also recognized in other geochronological studies that used different chronometers. For example, a recent Lu–Hf and Sm–Nd study documented *c.* 386–370 Ma ages for (U)HP granulites and closely associated middle crustal metapelites from the Stary Gierałtów area (Anczkiewicz *et al.* 2007). In addition, 370–360 Ma ages have also been reported for different occurrences of gneisses, leucosomes and granulites (e.g. Bröcker, Cosca & Klemd, 1997; Klemd & Bröcker, 1999; Štípská, Schulmann & Kröner, 2004; Gordon *et al.* 2005; Lange *et. al.* 2005*a*), but the geological significance remained unclear, due to methodological limitations of the dating techniques used and/or difficulties in linking age information with a specific *P–T* stage. In contrast to the granulites, previous geochronology did not establish convincing evidence for pre-350 Ma (U)HP processes affecting eclogites and associated gneisses. The new U–Pb data allow the reasoned inference that zircons of eclogites may record variable degrees of metamorphic crystal-chemical changes and/or new mineral growth between 390 and 360 Ma. It is tempting to speculate that these processes reflect (U)HP conditions, as suggested for the granulites of the Orlica-Śnieżnik complex, but there is yet no conclusive evidence to support this hypothesis.

Numerous studies have documented the importance of a *c.* 340 Ma event for the metamorphic evolution of the Orlica-Śnieżnik complex (e.g. Brueckner, Medaris & Bakun-Czubarow, 1991; Steltenpohl *et al.* 1993; Klemd & Bröcker, 1999; Turniak, Mazur & Wysoczanski, 2000; Marheine *et al.* 2002; Lange *et al.* 2002, 2005*a*,*b*; Štípská, Schulmann & Kröner, 2004; Bröcker *et al.* 2009). The new U–Pb ages for type 2 and 3 zircons mostly cluster at 330–350 Ma and further accentuate the importance of Carboniferous metamorphism. Similar zircon ages (SHRIMP, ID-TIMS, Pb–Pb evaporation) were also reported for an eclogite from Nowa Morawa (Bröcker *et al.* 2009) and granulites from the Červený Důl and Stary Gierałtów areas (Štípská, Schulmann & Kröner, 2004; Lange *et al.* 2005*a*; Anczkiewicz *et al.* 2007). The new U–Pb ages closely correspond to results obtained by other chronometric methods for the same rocks or different samples from the same outcrops. For sample NW-1, Bröcker *et al*. (2009) reported Rb–Sr and Sm–Nd mineral ages of 346.3 ± 4.2 Ma and 352.2 ± 3.4 Ma, respectively. ^{40}Ar–^{39}Ar and Rb–Sr phengite dating of sample 1111 yielded ages of *c.* 348 Ma and 331.3 ± 6.5 Ma, respectively. A different eclogite sample which was taken from the same outcrop as sample 5301 provided ^{40}Ar–^{39}Ar and Rb–Sr phengite ages of *c.* 349 Ma and of 330.9 ± 4.9 Ma. An eclogite sample collected close to the outcrop from which sample 5302 was taken yielded ^{40}Ar–^{39}Ar and Rb–Sr phengite ages of *c.* 348 Ma and 327.3 ± 4.1 Ma.

The geological significance of Carboniferous ages recorded in eclogites and granulites is controversial and has either been related to peak (U)HP conditions (e.g. Brueckner, Medaris & Bakun-Czubarow, 1991; Štípská, Schulmann & Kröner, 2004; Lange *et al.* 2005*a*), the waning stages of eclogite-facies metamorphism (e.g. Bröcker *et al.* 2009) or the amphibolite-facies overprint (Anczkiewicz *et al.* 2007). This controversy arises mainly because Sm–Nd ages do not allow unambiguous distinction between late HP metamorphism and amphibolite-facies overprinting, due to overlapping temperatures for both stages that are close to the closure temperature of garnet. Our study provides new arguments for this discussion, because the REE compositions of metamorphic zircon from both rock types strongly suggest contemporaneous crystallization of zircon and garnet. This interpretation is based on the observation of very low total REE abundances, flat HREE patterns, and the absence of an Eu anomaly. All these features strongly point to zircon formation under eclogite-facies conditions (e.g. Rubatto, 2002; Rubatto & Hermann, 2003; Whitehouse & Platt, 2003). The slight negative Eu-anomaly of type 2 and 3 zircon grains from the granulite sample 5312 (Fig. 8g) is interpreted as an inherited feature. Contemporaneous zircon and garnet growth during amphibolite-facies overprinting is unlikely because only one generation of garnet has been recognized in eclogites and granulites (e.g. Bröcker & Klemd, 1996; Perchuk *et al.* 2005). For granulites, Anczkiewicz *et al.* (2007) reported variable preservation of original prograde garnet growth zoning that has been modified by diffusional homogenization creating flat compositional profiles, and minor compositional changes at garnet rims due to partial re-equilibration with matrix phases. Such intra- and intergrain diffusional processes would not affect the REE charcteristics of newly grown zircon. Non-cogenetic garnet generations with distinct chemical compositions were not recognized. Trace element characteristics suggest that zircon growth in both eclogites and granulites can be linked to a HP episode. U–Pb dating of such zircon grains indicates a Carboniferous age for this *P–T* stage. This does not rule out the possibility that similar Variscan ages of the orthogneisses may record a different metamorphic regime that was attained at the same time in other parts of the orogen.

https://doi.org/10.1017/S0016756809990665 Published online by Cambridge University Press

6.e. Ti-in-zircon thermometry

Ti-in-zircon thermometry (Watson, Wark & Thomas, 2006) is based on experiments performed at 10 kbar, and is dependent on activities of SiO_2 and TiO_2, and pressure (Ferry & Watson, 2007). In the studied samples, crystallization of magmatic zircon most likely occurred in the presence of quartz and ilmenite ($a_{SiO2} = 1$ and $a_{TiO2} = 0.6$) at pressures broadly approximated by the experimental conditions. For zircons of CL types 1 and 4, Ti-in-zircon thermometry (Ferry & Watson, 2007; Table 3) indicates apparent temperatures of *c.* 790–870 °C that are lower than crystallization temperatures of basic melts. Lower than expected Ti-in-zircon temperatures may indicate late stage zircon growth in evolved magmatic systems (e.g. Kaczmarek, Müntener & Rubatto, 2008), but other processes influencing the incorporation of Ti into zircon have also been shown to induce a similar effect (Fu *et al.* 2008). Thus, caution is warranted in applying Ti-in-zircon thermometry, because many aspects of this method are not yet fully understood (e.g. Fu *et al.* 2008). For example, Ferriss, Essene & Becker (2008) questioned the reliability of the Ti-in-zircon thermometer for UHP rocks, because under such conditions, Ti substitution into the Zr instead of the Si site becomes more important. In the studied eclogites and granulites, metamorphic zircon formed in the presence of quartz and rutile ($a_{SiO2} = 1$ and $a_{TiO2} = 1$) at high to ultrahigh pressure conditions. Ferry & Watson (2007) suggested for the Ti thermometer a pressure correction of 5 °C/kbar at 750 °C, but quantum-mechanical calculations (Ferriss, Essene & Becker, 2008) predict that the necessary pressure correction should be twice as large. Such corrections were not applied, because zircon growth can only broadly be linked to eclogite-facies conditions, but not to a specific pressure. As a result, metamorphic temperatures may be underestimated by *c.* 50–130 °C at pressures between 15 and 28 kbar. Ti-in-zircon temperatures for metamorphic zircon of eclogites, uncorrected for pressure, fall within the range of 690–820 °C that has been estimated for these rocks using conventional geothermometry (e.g. Bakun-Czubarow, 1991*a*,*b*; Bröcker & Klemd, 1996). Similarily, for the granulite sample 5312, Ti-in-zircon thermometry indicates metamorphic temperatures of about 885 °C, conforming to the previously estimated 800–1000 °C range.

7. Conclusions

Attempts to determine accurate and precise protolith ages for eclogites and granulites from the Orlica-Śnieżnik complex have been severely hampered by variable degrees of isotopic resetting that affected the U–Pb isotope system of individual zircon grains. For both rock types, SHRIMP and LA-ICPMS data show a large spread in apparent U–Pb ages, and a younging trend towards 330–340 Ma, which is the well-established age of Variscan metamorphism in the study area. Pb-loss is considered as the most important cause for this age variability. The disturbance of the U–Pb zircon system is observed in samples representing different *P–T* paths, and can be related to two processes: partial metamictization and/or protracted metamorphism. The individual contributions of these processes to the overall result and their timing are difficult to assess. In the case of the eclogites, radiation damage in combination with metamorphic overprinting is considered to be the dominant factor for post-crystallization disturbance of the isotope system. In the case of the granulites, exposure of these rocks to protracted or multiple HT metamorphism may have produced favourable circumstances to induce partial resetting of non-metamict zircon. The exact age relationships between (U)HP rocks and their host rocks (coeval, younger or older country rocks) remains unresolved.

The last metamorphic overprint at *c.* 350–330 Ma represents a major episode of new zircon growth and other crystal-chemical changes affecting this phase. The contributions of earlier metamorphic events have yet to be resolved. In eclogites a conspicuous data cluster at *c.* 360–380 Ma was recognized. It is not understood whether this feature indicates metamorphic processes similar to those indicated by Lu–Hf dating of the granulites (Anczkiewicz *et al.* 2007) or a fortuitous accumulation of dates representing incompletely reset grains. U–Pb zircon ages of *c.* 330–350 Ma complement existing datasets that, at least for the eclogites, are largely based on other chronometers. Trace element characteristics of metamorphic zircon from both eclogites and granulites suggest contemporaneous crystallization with garnet, supporting interpretations that relate Carboniferous ages in (U)HP rocks to late-stage eclogite-facies metamorphism and not to middle crustal overprinting.

Acknowledgements. This study was funded by the Deutsche Forschungsgemeinschaft (grant BR 1068/11-1). Reviews by S. Mazur and an anonymous referee are greatly appreciated. Supplementary online Appendix is available at http://journals.cambridge.org/geo.

References

ANCZKIEWICZ, R., SZCZEPAŃSKI, J., MAZUR, S., STOREY, C., CROWLEY, Q., VILLA, I. M., THIRLWALL, M. F. & JEFFRIES, T. E. 2007. Lu–Hf geochronology and trace element distribution in garnet: Implications for uplift and exhumation of ultra-high pressure granulites in the Sudetes, SW Poland. *Lithos* **95**, 363–80.

ASHWAL, L. D., TUCKER, R. D. & ZINNER, E. K. 1999. Slow cooling of deep crustal granulites and Pb-loss in zircon. *Geochimica et Cosmochimica Acta* **63**, 2839–51.

BAKUN-CZUBAROW, N. 1968. Geochemical characteristics of eclogites from the environs of Nowa Wieś in the region of Śnieżnik Kłodzki. *Archiwum Mineralogiczne* **28**, 244–371.

https://doi.org/10.1017/S0016756809990665 Published online by Cambridge University Press

BAKUN-CZUBAROW, N. 1991*a*. On the possibility of quartz pseudomorphs after coesite in the eclogite-granulite rock series of the Złote Mountains in the Sudetes (SW Poland). *Archiwum Mineralogiczne* **42**, 5–16.

BAKUN-CZUBAROW, N. 1991*b*. Geodynamic significance of the Variscan HP eclogite-granulite series of the Złote Mountains in the Sudetes. *Publications of the Institute of Geophysics, Polish Academy of Sciences* **A-19**(236), 215–42.

BAKUN-CZUBAROW, N. 1992. Quartz pseudomorphs after coesite and quartz exsolutions in eclogite omphacites of the Złote Mountains in the Sudetes (SW Poland). *Archiwum Mineralogiczne* **48**, 3–25.

BAKUN-CZUBAROW, N. 1998. Ilmenite-bearing eclogites of the West Sudetes – their geochemistry and mineral chemistry. *Archiwum Mineralogiczne* **51**, 29–110.

BLACK, L. P., KAMO, S. L., ALLEN, C. M., ALEINIKOFF, J. N., DAVIS, D. W., KORSCH, R. J. & FOUDOULIS, C. 2003. TEMORA 1: a new zircon standard for Phanerozoic U–Pb geochronology. *Chemical Geology* **200**, 155–70.

BOYNTON, W. V. 1984. Cosmochemistry of the rare earth elements: meteorite studies. In *Rare Earth Element Geochemistry* (ed. P. Henderson), pp. 63–114. Developments in Geochemistry 2. Amsterdam: Elsevier.

BRÖCKER, M., COSCA, M. & KLEMD, R. 1997. Geochronologie von Eklogiten und assoziierten Nebengesteinen des Orlica–Snieznik Kristallins (Sudeten, Poland): Ergebnisse von U–Pb, Sm–Nd, Rb–Sr und Ar–Ar Untersuchungen. *Terra Nostra* **97**(5), 29–30.

BRÖCKER, M. & KLEMD, R. 1996. Ultrahigh-pressure metamorphism in the Śnieżnik Mountains (Sudetes, Poland): P–T constraints and geological implications. *Journal of Geology* **104**, 417–33.

BRÖCKER, M., KLEMD, R., COSCA, M., BROCK, W., LARIONOV, A. N. & RODIONOV, N. 2009. The timing of eclogite-facies metamorphism and migmatization in the Orlica-Śnieżnik complex, Bohemian Massif: constraints from a geochronological multi-method study. *Journal of Metamorphic Geology* **27**, 385–403.

BRUECKNER, H. K., MEDARIS, L. G. JR & BAKUN-CZUBAROW, N. 1991. Nd and Sr age and isotope patterns from Variscan eclogites of the eastern Bohemian Massif. *Neues Jahrbuch für Mineralogie, Abhandlungen* **163**, 169–96.

CHERNIAK, D. J. & WATSON, E. B. 2001. Pb diffusion in zircon. *Chemical Geology* **172**, 5–24.

COMPSTON, W., WILLIAMS, I. S. & MEYER, C. 1984. U–Pb geochronology of zircons from the lunar breccia 73217 using a sensitive high-resolution ion microprobe. *Journal of Geophysical Research* **89**, B525–34.

DON, J. 2001. The relationship between the Gierałtów migmatites and the Śnieżnik granitogneisses within the Kletno fold. *Mineralogical Society of Poland, Special Papers* **19**, 189–93.

DON, J., DUMICZ, M., WOJCIECHOWSKA, I. & ŻELAŹNIEWICZ, A. 1990. Lithology and tectonics of the Orlica-Śnieżnik Complex, Sudetes – recent state of knowledge. *Neues Jahrbuch für Geologie und Paläontologie, Abhandlungen* **179**, 159–88.

DUMICZ, M. 1993. The history of eclogites in the geological evolution of the Śnieżnik crystalline complex based on mesostructural analysis. *Geologia Sudetica* **27**, 21–48.

FERRISS, E. D. A., ESSENE, E. J. & BECKER, U. 2008. Computanional study of the effects of pressure on the Ti-in-zircon geothermometer. *European Journal of Mineralogy* **20**, 745–55.

FERRY, J. M. & WATSON, E. B. 2007. New thermodynamic models and revised calibrations for the Ti-in-zircon and Zr-in-rutile thermometers. *Contributions to Mineralogy and Petrology* **154**, 429–37.

FU, B., PAGE, F. Z., CAVOSIE, A. J., FOURNELLE, J., KITA, N. T., LACKEY, J. S., WILDE, S. A., & VALLEY, J. W. 2008. Ti-in-zircon thermometry: applications and limitations. *Contributions to Mineralogy and Petrology* **156**, 197–215.

GEHRELS, G. E., VALENCIA, V. & PULLEN, A. 2006. Detrital zircon geochronology by laser ablation multicollector ICPMS at the Arizona LaserChron Center. In *Geochronology: Emerging Opportunities* (ed. T. Olszewski), pp. 67–76. Paleontological Society Short Course, Philadelphia, PA.

GORDON, S. M., SCHNEIDER, D. A., MANECKI, M. & HOLM, D. K. 2005. Exhumation and metamorphism of an ultrahigh-grade terrane: geochronometric investigations of the Sudete Mountains (Bohemia), Poland and Czech Republic. *Journal of the Geological Society, London* **162**, 841–55.

GRIFFIN, W., POWELL, W. J., PEARSON, N. J. & O'REILLY, S. Z. 2008. Glitter: Data Reduction Software For Laser Ablation ICP-MS. In *Laser Ablation ICP-MS in the Earth Sciences: Current Practices and Outstanding Issues* (ed. P. Sylvester), Appendix 2, pp. 308–11. Mineralogical Association of Canada, Short Course Series 40.

HARLEY, S. L., KELLY, N. M. & MÖLLER, A. 2007. Zircon behaviour and the thermal histories of mountain chains. *Elements* **3**, 25–30.

JACKSON, S., PEARSON, N. J., GRIFFIN, W. L. & BELOUSOVA, E. A. 2004. The application of laser ablation-inductively coupled plasma-mass spectrometry to in situ U–Pb zircon geochronology. *Chemical Geology* **211**, 47–69.

KACZMAREK, M.-A., MÜNTENER, O. & RUBATTO, D. 2008. Trace element chemistry and U–Pb dating of zircons from oceanic gabbros and their relationship with whole rock composition (Lanzo, Italian Alps). *Contributions to Mineralogy and Petrology* **155**, 295–312.

KLEMD, R. & BRÖCKER, M. 1999. Fluid influence on mineral reactions in ultrahigh-pressure granulites: a case study in the Śnieżnik Mts. (West Sudetes, Poland). *Contributions to Mineralogy and Petrology* **136**, 358–73.

KLEMD, R., BRÖCKER, M. & SCHRAMM, J. 1995. Characterization of amphibolite-facies fluids of Variscan eclogites from the Orlica-Śnieżnik dome (Sudetes, SW Poland). *Chemical Geology* **119**, 101–13.

KOGLIN, N., KOSTOPOULOS, D. & REISCHMANN, T. 2008. The Lesvos mafic–ultramafic complex, Greece: ophiolite or incipient rift? *Lithos* **108**, 243–61.

KRÖNER, A., JAECKEL, P., HEGNER, E. & OPLETAL, M. 2001. Single zircon ages and whole-rock Nd isotopic systematics of early Palaeozoic granitoid gneisses from the Czech and Polish Sudetes (Jizerské hory, Krkonoše Mountains and Orlice-Sněžník Complex). *International Journal of Earth Sciences (Geologische Rundschau)* **90**, 304–24.

KRYZA, R., PIN, C. & VIELZEUF, D. 1996. High-pressure granulites from the Sudetes (south-west Poland): evidence of crustal subduction and collisional thickening in the Variscan Belt. *Journal of Metamorphic Geology* **14**, 531–46.

LANGE, U., BRÖCKER, M., ARMSTRONG, R., TRAPP, E. & MEZGER, K. 2005*a*. Sm–Nd and U–Pb dating of high-pressure granulites from the Złote and Rychleby Mts (Bohemian Massif, Poland and Czech Republic). *Journal of Metamorphic Geology* **23**, 133–45.

LANGE, U., BRÖCKER, M., ARMSTRONG, R., ŻELAŹNIEWICZ, A., TRAPP, E. & MEZGER, K. 2005*b*. The orthogneisses

of the Orlica-Śnieżnik complex (West Sudetes, Poland): geochemical characteristics, the importance of pre-Variscan migmatization and constraints on the cooling history. *Journal of the Geological Society, London* **162**, 973–84.

LANGE, U., BRÖCKER, M., MEZGER, K. & DON, J. 2002. Geochemistry and Rb–Sr geochronology of a ductile shear zone in the Orlica-Śnieżnik complex (West Sudetes, Poland). *International Journal of Earth Sciences (Geologische Rundschau)* **91**, 1005–16.

LARIONOV, A. N., ANDREICHEV, V. A. & GEE, D. G. 2004. The Vendian alkaline igneous suite of northern Timan: ion microprobe U–Pb zircon ages of gabbros and syenite. In *The Neoproterozoic Timanide Orogen of Eastern Baltica* (eds D. G. & V. L. Pease), pp. 69–74. Geological Society of London, Memoir no. 30.

LEE, J. K. W., WILLIAMS, I. S. & ELLIS, D. J. 1997. Pb, U and Th diffusion in natural zircon. *Nature* **390**, 159–62.

LUDWIG, K. R. 2005*a*. *SQUID 1.12 A User's Manual. A Geochronological Toolkit for Microsoft Excel*. Berkeley Geochronology Center Special Publication, 22 pp. World Wide Web Address: http://www.bgc.org/klprogrammenu.html.

LUDWIG, K. R. 2005*b*. *User's Manual for ISOPLOT/Ex 3.22. A Geochronological Toolkit for Microsoft Excel*. Berkeley Geochronology Center Special Publication, 71 pp.

MARHEINE, D., KACHLIK, V., MALUSKI, H., PATOCKA, F. & ŻELAŹNIEWICZ, A. 2002. The $^{40}Ar/^{39}Ar$ ages from the West Sudetes (NE Bohemian Massif); constraints on the Variscan polyphase tectonothermal development. In *Paleozoic amalgamation of Central Europe* (eds J. A. Winchester, T. V. Pharaoh & J. Verniers), pp. 133–55. Geological Society of London, Special Publication no. 201.

OLIVER, G. J. H., CORFU, F. & KROGH, T. E. 1993. U–Pb ages from SW Poland: evidence for a Caledonian suture zone between Baltica and Gondwana. *Journal of the Geological Society, London* **150**, 355–69.

PERCHUK, L. L., KORCHAGINA, M. A., YAPASKURT, V. O. & BAKUN-CZUBAROW, N. 2005. Some High-Pressure Metamorphic Complexes in the West Sudetes, Poland: I. Petrography and Mineral Chemistry. *Petrology* **13**(5), 427–68.

PEYTCHEVA, I., VON QUADT, A., GEORGIEV, N., IVANOV, ZH., HEINRICH, C. A. & FRANK, M. 2008. Combining trace-element compositions, U–Pb geochronology and Hf isotopes in zircons to unravel complex calcalkaline magma chambers in the Upper Cretaceous Srednogorie zone (Bulgaria). *Lithos* **104**, 405–27.

PILOT, J., WERNER, C.-D., HAUBRICH, F. & BAUMANN, N. 1998. Palaeozoic and proterozoic zircons from the Mid-Atlantic Ridge. *Nature* **393**, 676–9.

POUBA, Z., PADĚRA, K. & FIALA, J. 1985. Omphacite granulite from the NE marginal area of the Bohemian Massif (Rychleby Mts). *Neues Jahrbuch für Mineralogie, Abhandlungen* **151**, 29–52.

PRESNYAKOV, S., LEPEKHINA, E., BELYATSKY, B., SHULIATIN, O., ANTONOV, A. & SERGEEV, S. 2008. Accessory zircon from the modern oceanic crust. *33rd International Geological Congress Oslo*, *Abstract Volume*, MPC01224P.

PRESSLER, R. E., SCHNEIDER, D. A., PETRONIS, M. S., HOLM, D. K. & GEISSMAN, J. W. 2007. Pervasive horizontal fabric and rapid vertical extrusion: Lateral overturning and margin sub-parallel flow of deep crustal migmatites, northeastern Bohemian Massif. *Tectonophysics* **443**, 19–36.

ROOT, D. B., HACKER, B. R., MATTINSON, J. M. & WOODEN, J. L. 2004. Zircon geochronology and ca. 400 Ma exhumation of Norwegian ultrahigh-pressure rocks: an ion microprobe and chemical abrasion study. *Earth and Planetary Science Letters* **228**, 325–41.

RUBATTO, D. 2002. Zircon trace element geochemistry: distribution coefficients and the link between U–Pb ages and metamorphism. *Chemical Geology* **184**, 123–38.

RUBATTO, D. & HERMANN, J. 2003. Zircon formation during fluid circulation in eclogites (Monviso, Western Alps): implications for Zr and Hf budget in subduction zones. *Geochimica et Cosmochimica Acta* **67**, 2173–87.

SCHNEIDER, D. A., ZAHNISER, S., GLASCOCK, J., GORDON, S. M. & MANECKI, M. 2006. Thermochronology of the West Sudetes (Bohemian Massif): rapid and repeated eduction in the eastern Variscides, Poland and Czech Republic. *American Journal of Science* **306**, 846–73.

SLÁMA, J., KOŠLER, J., CONDON, D. J., CROWLEY, J. L., GERDES, A., HANCHAR, J. M., HORSTWOOD, M. S. A., MORRIS, G. A., NASDALA, L., NORBERG, N., SCHALTEGGER, U., SCHOENE, B., TUBRETT, M. N. & WHITEHOUSE, M. J. 2008. Plešovice zircon – A new natural reference material for U–Pb and Hf isotopic microanalysis. *Chemical Geology* **249**, 1–35.

SMULIKOWSKI, K. 1967. Eclogites of the Śnieżnik Mountains in the Sudetes. *Geologia Sudetica* **3**, 7–180.

SMULIKOWSKI, K. & SMULIKOWSKI, W. 1985. On the porphyroblastic eclogites of the Śnieżnik Mountains in the Polish Sudetes. *Chemical Geology* **50**, 201–22.

STACEY, J. S. & KRAMERS, J. D. 1975. Approximation of terrestrial lead isotope evolution by a two-stage model. *Earth and Planetary Science Letters* **26**, 207–21.

STEIGER, R. H. & JÄGER, E. 1977. Subcommission on geochronology: convention on the use of decay constants in geo- and cosmochronology. *Earth and Planetary Science Letters* **36**, 359–62.

STELTENPOHL, M. G., CYMERMAN, Z., KROGH, E. J. & KUNK, M. J. 1993. Exhumation of eclogitized continental basement during Variscan lithospheric delamination and gravitational collapse, Sudety Mountains, Poland. *Geology* **21**, 1111–14.

ŠTÍPSKÁ, P., SCHULMANN, K. & KRÖNER, A. 2004. Vertical extrusion and middle crustal spreading of omphacite granulite: a model of syn-convergent exhumation (Bohemian Massif, Czech Republic). *Journal of Metamorphic Geology* **22**, 179–98.

SYLVESTER, P. J. & GHADERI, M. 1997. Trace element analysis of scheelite by excimer laser ablation inductively coupled plasma mass spectrometry (ELA-ICP-MS) using a synthetic glass standard. *Chemical Geology* **141**, 49–65.

TURNIAK, K., MAZUR, S. & WYSOCZANSKI, R. 2000. SHRIMP zircon geochronology and geochemistry of the Orlica-Śnieżnik gneisses (Variscan belt of Central Europe) and their tectonic implications. *Geodinamica Acta* **13**, 293–312.

WATSON, E. B., WARK, D. & THOMAS, J. 2006. Crystallization thermometers for zircon and rutile. *Contributions to Mineralogy and Petrology* **151**, 413–33.

WHITEHOUSE, M. J. & PLATT, J. P. 2003. Dating high-grade metamorphism: constraints from rare-earth elements in zircon and garnet. *Contributions to Mineralogy and Petrology* **145**, 61–74.

WIEDENBECK, M., ALLÉ, P., CORFU, F., GRIFFIN, W. L., MEIER, M., OBERLI, F., VON QUADT, A., RODDICK, J. C. & SPIEGEL, W. 1995. Three natural zircon standards for U-Th-Pb, Lu–Hf, trace element and REE analyses. *Geostandards Newsletter* **19**, 1–23.

WILLIAMS, I. S. 1998. U–Th–Pb geochronology by ion microprobe. In *Applications of microanalytical techniques to understanding mineralizing processes* (eds M. A. McKibben, W. C. Shanks III & W. I. Ridley), pp. 1–35. *Reviews in Economic Geology* **7**.

ŻELAŹNIEWICZ, A., MAZUR, S. & SZCZEPAŃSKI, J. 2002. The Lądek-Śnieżnik Metamorphic Unit – recent state of knowledge. *Geolines* **14**, 115–25.

ŻELAŹNIEWICZ, A., NOWAK, I., LARIONOV, A. N. & PRESNYAKOV, S. 2006. Syntectonic lower Ordovician migmatite and post-tectonic Upper Viséan syenite in the western limb of the Orlica-Śnieżnik Dome, West Sudetes: U–Pb SHRIMP data from zircons. *Geologia Sudetica* **38**, 63–80.

https://doi.org/10.1017/S0016756809990665 Published online by Cambridge University Press